HYDRAULIC RESPONSE TO EMULSIFIED VEGETABLE OIL BIOSTIMULATION: IN-SITU TEST IN A HIGHLY HETEROGENOUS URANIUM CONTAMINATED AQUIFER

A Thesis Presented for the
Master of Science
Degree
The University of Tennessee, Knoxville

Benjamin Gregory Adams
May 2019

Copyright © 2019 by Benjamin G. Adams
All rights reserved.

ACKNOWLEDGEMENTS

First, I would like to acknowledge my advisor and mentor Dr. Terry Hazen. In 2014 he allowed me to join his lab as an undergraduate research assistant. This allowed me to gain valuable hands-on experience in both the field and the laboratory. Shortly after graduating with my bachelor's degree, he invited me to continue my education in graduate school. He has been a source of inspiration, knowledge, and guidance through my graduate studies to ensure that I am prepared for the future.

I would also like to acknowledge my two committee members, Dr. Larry McKay and Dr. Annette Engel. Dr. McKay supported the evolution of this thesis by encouraging me to think critically and provided guidance to steer me in the right direction. One of my first graduate courses was with Dr. Engel. The enthusiasm and interest she showed in this course lead me to become more interested in aqueous geochemistry and enjoy the challenges of addressing environmental problems. I would also like to recognize Dr. Ed Perfect whose guidance regarding statistical analysis gave me the knowledge I needed to understand the results of my experiment. I will extend a special recognition to Kenneth Lowe who helped me learn my way around ORNL and was always there if help was needed. I would like to thank Kathyrn McBride for being an excellent and reliable partner through the many sampling days with horrible weather, and the nice days (there weren't many). Also, I would like to thank all of the members of Hazen Lab for their support and motivation.

The field sampling, geochemical, and microbial analysis was supported by ENIGMA-Ecosystems and Networks Integrated with Genes and Molecular Assemblies, a

Scientific Focus Area Program at Lawrence Berkeley National Laboratory, under Contract No. DE-AC02-05CH11231 through the Office of Science, Office of Biological and Environmental Research, of the US Department of Energy.

Finally, I would like to thank my family for their support and encouragement throughout my time at UTK. Most of all, I would like to extend a special thank you to my wife Jade. She has been extremely supportive, patient, and understanding through my education and none of this would have been possible without her.

ABSTRACT

The purpose of this study was to determine if the injection of emulsified vegetable oil (EVO) to remediate a uranium-contaminated aquifer can result in a reduction in hydraulic conductivity. The secondary purpose was to determine if there was evidence of a "memory effect," a phenomenon where the second time an electron donor is injected, the environment responds to it faster. This has been observed at many remediation sites. A previously treated (2009) uranium contaminated aquifer at Y-12 National Security Complex located in Oak Ridge, Tennessee, was injected with EVO to determine whether hydraulic conductivity changes and to assess the effectiveness of EVO treatment for reducing dissolved uranium. Acetate was monitored in downgradient wells as an indicator of biodegradation. On December 13, 2017, a 20% EVO and groundwater mixture was injected within the Y-12 FRC Area 2 site. Periodic measurements of hydraulic conductivity and dissolved uranium concentration were taken from a control wells, three injection wells, and four down-gradient wells for 134 days. During the experiment, hydraulic conductivity in the injection wells decreased by up to two orders of magnitude but only up to one order of magnitude in half of the down-gradient monitoring wells located 2.5 to 11 m away. Dissolved uranium concentrations significantly decreased in the injection wells, but not in the monitoring well directly down-gradient of injection because dissolved uranium concentrations increased by day 78 and surpassed pre-injection concentrations due to oxidation of reduced uranium in those wells. Acetate concentrations indicated an accelerated response to EVO compared to the 2009 study results. However, this was the only evidence of "memory response." The results of this study show that injecting EVO can

have unintended consequences related to hydraulic conductivity, which can reduce EVO effectiveness or even cause bioremediation using EVO to fail. The effects of EVO interacting with aquifer media and injection well spacing should be carefully considered to minimize changes in preferential flow, limit oxidation of reduced uranium, and maximize the effectiveness of the treatment.

TABLE OF CONTENTS

Chapter One Introduction and Background 1
Chapter Two Literature Review: Changes in Hydraulic Conductivity Related to Electron Donor Injection 7
Amendment Effects 7
Water Table Fluctuations 12
Mineral Precipitation, and Dissolution 14
Fines and Colloids 15
Bioclogging and Microbial Effects 16
Chapter Three Site Background, Goals, Objectives, and Hypotheses 18
Site Background 18
Goals 25
Objectives and Hypothesis 25
Chapter Four Materials and Methods 28
Summary of Injection and Sampling Schedule 28
Well Inspection and Preparation 30
Emulsified Vegetable Oil (EVO) Source and Composition 31
EVO Preparation and Injection 31
Measuring Hydraulic Conductivity 32
Sampling Method 36
HPLC and ICP-MS Sample Analysis 36
Statistical Analysis 37
Chapter Five Results and Discussion 41
Groundwater Elevation (GWE) 41
Hydraulic Gradient 45
Hydraulic Conductivity 45
Dissolved Uranium Concentrations 55
Post-injection Down-gradient Acetate Concentrations 60
Correlations 62
Chapter Six Summary and Conclusions 66
List of References 72
Vita 78

LIST OF TABLES

Table 1. Reported values for hydraulic conductivity (cm/s) in Area 2 and other sites in Bear Creek Valley with similar geology. Locations other than Area 2 consist of wells screened in intact saprolite or regolith overlying it rather than the reworked saprolite and gravel fill present in Area 2. Bedrock refers to the underlying Nolichucky Shale [2, 11, 42, 43, 48-50]. 20
Table 2. An outline of the field work schedule followed during the experiment. 29
Table 3. Composition of EVO solution used for injection. 31
Table 4. Well construction data used to calculate hydraulic conductivity. 35
Table 5. Pumping rates and drawdown used to calculate the hydraulic conductivity in injection wells. 46
Table 6. Pumping rates and drawdown used to calculate hydraulic conductivity in the control and monitoring wells. 47
Table 7. Normalized hydraulic conductivity values. Each well has been normalized against the pre-injection value (day -6). Normalization removes the influence of spatial variation and allows for the comparison of change relative to the pre-injection measurement. 51
Table 8. The reported two-tail p-values of paired t-tests comparing normalized post-injection hydraulic conductivity values of the control well to the other wells used in the study. Statistically significant results have been highlighted in bold. 52
Table 9. Normalized dissolved uranium concentrations. Each well has been normalized against the pre-injection concentration (day -6). Normalization removes the influence of spatial variation and allows for the comparison of change relative to the pre-injection 58
Table 10. The reported two-tail p-values of paired t-tests comparing normalized post-injection dissolved uranium concentrations of the control well to the other wells used in the study. Statistically significant results have been highlighted in bold..... 59
Table 11. Acetate concentrations (μM) in the control and down-gradient monitoring wells over the course of the experiment. An entry of BD means the sample was below the detection limit of the instrument. 63
Table 12. A correlation matrix computed using the Kendall method and pair-wise deletions. The number of asterisks indicate significance level (p-value) of the relationship. Three significance levels are present: p-value ≤ 0.0001 (***), p-value ≤ 0.001 (**), and p-value ≤ 0.01 (*). Correlations with p-values ≤ 0.001 are highlighted with bold text. 64

LIST OF FIGURES

Figure 1. Terminal electron acceptors (TEA) and the succession during biostimulation. High concentrations of nitrate can prevent the environment from reaching conditions that are favorable for the reduction of U(VI) to U(IV) (after Hazen, 2018) [6]. 2
Figure 2. The effectiveness of biostimulation in relation to hydraulic conductivity (after Hazen, 2018 [6]). 9
Figure 3. A cross-section representative of the Area 2 sub-surface, not to scale (modified from Watson et al., 2013 [2]). 19
Figure 4. The Oak Ridge Field Research Center with typical groundwater quality and contamination levels for the areas around the former S-3 Ponds. The former S-3 Ponds are approximately 750 ft. (229 m) NE of the study site within Area 2. Wells labelled as "Saprolite Well" can be screened in either unconsolidated clay-rich fill or intact saprolite [42]. 22
Figure 5. Annotated Google Earth imagery of the former S-3 Ponds and the injection site. (Edited from Google Earth Pro 7.1.8.3036 (32-bit) (April 12, 2018). Oak Ridge, TN. 35°58'37.74" N, 84°16'24.48" W, Eye alt 643m. http://www.earth.google.com [September 26, 2018]). 23
Figure 6. Plan view map of the injection site. Surface contours are brown and labeled in units of meters above mean sea-level (mamsl). 24
Figure 7. Groundwater elevation (GWE) in meters above mean sea-level (mamsl) during the experiment. The red dashed line represents the day of injection. 42
Figure 8. Precipitation from six days before injection until the final day of the experiment. The red dashed line represents the date of injection. The heaviest period of precipitation occurred between day 45 and day 78. 44
Figure 9. A faceted graph of hydraulic conductivity during the study. Labels within each facet identify the well type. The red dashed line represents the day of injection. 49
Figure 10. A box and whisker plot of post-injection hydraulic conductivity values by well type. Control, injection, and monitoring wells were all significantly different ($p < 0.0001$) from each other. The control well had the highest average hydraulic conductivity and the injection wells had the lowest average hydraulic conductivity. 54
Figure 11. A faceted graph of dissolved uranium concentrations measured during the experiment. Each facet is labeled with the well type. The dashed red line represents the day of injection. Injection wells had concentrations lower than their pre-injection values at the end of the experiment. All monitoring wells were either near their pre-injection concentrations or surpassed them by the end of the study. 56
Figure 12. A box and whisker plot of dissolved uranium concentrations by well type. The control well had the highest average concentration and the injection wells had the lowest average concentration during the experiment. Monitoring wells had an average concentration that was approximately 500 µg/L higher than the injection wells. 61

CHAPTER ONE
INTRODUCTION AND BACKGROUND

Studies have shown that biostimulation using emulsified vegetable oil (EVO) can reduce the concentration of dissolved uranium in contaminated groundwater through bioimmobilization [1-4]. EVO as a substrate has many properties that contribute to its effectiveness. It is a slow-release substrate with a high electron donor density that can provide a sustained source of carbon, energy, and limiting nutrients within a treatment area. EVO stimulates indigenous microorganisms that can maintain suboxic or reducing redox state within the groundwater, which can promote the reduction of U(VI) to U(IV). Uranium in the U(VI) valence state is in aqueous phase and highly mobile in groundwater, while its reduced state, U(IV), is less mobile and can precipitate as uraninite under specific conditions.

Although use of EVO can reduce the concentration of dissolved uranium, repeated applications are necessary to maintain bioimmobilization conditions. The reduced effectiveness of treatment often results from inadequate distribution and contact between reagent and substrates [5]. If the initial iteration is unsuccessful at inducing bioimmobilization, then the result is an increase in time and cost required to meet conditions needed for successful treatment. However, it is unlikely that U(IV) persists for long periods of time due to factors like the influx of rainwater or high concentrations of nitrate that can reoxidized uranium and increase mobility. High nitrate concentrations can result in sustained denitrification and prevent conditions favorable for the reduction of U(VI) (**Figure 1**) [6]. It is also understood that the reintroduction of nitrate can lead to reoxidation of bioreduced U(IV) to U(VI) [7]. Bacterial U(VI) reduction is

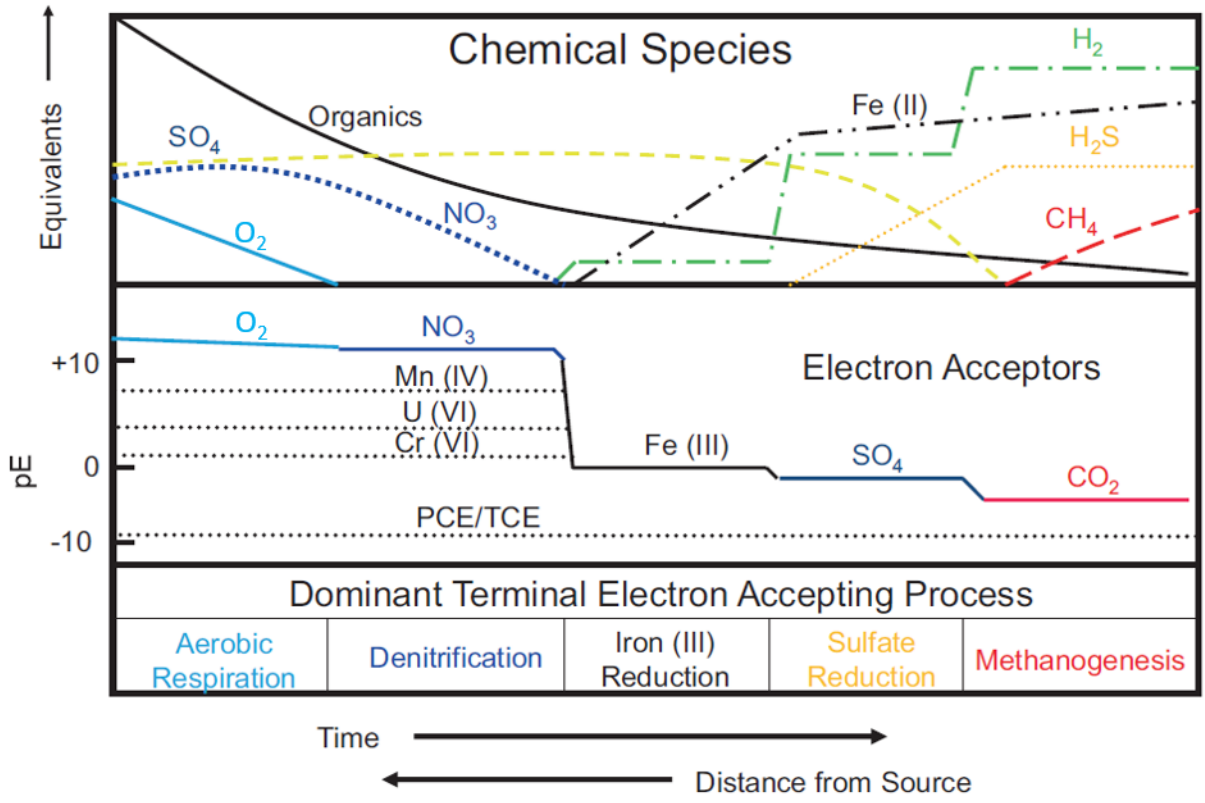


Figure 1. Terminal electron acceptors (TEA) and the succession during biostimulation. High concentrations of nitrate can prevent the environment from reaching conditions that are favorable for the reduction of U(VI) to U(IV) (after Hazen, 2018) [6].

inhibited by calcium [8], with a concentration of 5 mM [millimolar] being enough to inhibit U(VI) reduction.

Emerging evidence has shown that exposure history of a groundwater zone to a supplemented electron donor can have a lasting positive effect on biodegradation rate, referred to as “memory effect” [9-11]. This concept is suggested to be responsible for the relatively quick amelioration of the *Deepwater Horizon* oil spill in the deep-water plume [12]. An increased biodegradation response could significantly increase the timing of iron reduction and the conditions necessary for reducing dissolved uranium. If the “memory response” were better understood, then the timing of subsequent injections can more effectively planned to maintain the conditions necessary to keep uranium immobilized.

In a fractured or granular media, reductions in hydraulic conductivity can result in inadequate dispersion of an injected amendment, like EVO, which can cause contaminated groundwater to flow around the treatment zone [13]. These changes can occur due to amendment effects that result from physical properties of the amendment, such as viscosity, specific gravity, droplet size variation, composition, and also from how these amendment properties interact with aquifer media [13-15]. Conditions may change, such that hydraulic conductivity increases, that result from dissolution of minerals in pore space and fractures [16, 17]. This can impact flow and lead to a much faster rate of dispersion and decreased residence time, which can ultimately reduce the effectiveness of the treatment. In contrast, geochemical conditions can become favorable for precipitation of minerals, which would reduce available pore volume, or entirely close pore throats, and lead to significant reduction in hydraulic conductivity. These reductions can result in increased residence time of groundwater within the treatment location and possibly

impact the ability of an amendment, like EVO, to disperse throughout the target area and contaminated groundwater to flow through the treatment zone. In some instances, an increase in residence time may be beneficial, as this would likely allow oxygen and nitrate to be depleted so that conditions become favorable for U(VI) reduction. However, if these conditions are quickly met, or oxygen and nitrate are already depleted, then the amendment may be degraded, but contaminated groundwater would flow around the injection area. Both effects can lead to decreased treatment efficiency and may result in unforeseen changes in the preferential flow of groundwater within a treatment area. Conversely, if the amendment is degraded rapidly due to an increased response rate from previous exposures to EVO, then the time scales related to precipitation and dissolution may only be relevant in the context of the mobilization and bioimmobilization contaminants.

Bioclogging is another possible factor that may lead to a decrease of hydraulic conductivity. The introduction of EVO can result in increased proliferation of bacteria and their associated biofilms since growth is no longer limited by organic carbon and electron donors. In the context of "memory response," the proliferation and growth of biofilms can occur more quickly with subsequent injections. Biofilms form on fracture networks and within pore spaces that would result in a decrease in effective porosity and a reduction in hydraulic conductivity [18-22].

Before injection, EVO is mixed with local groundwater to create a solution rather than simply injecting the amendment on its own. The removal of groundwater can release fines and colloids into the system, which can result in reduced pore volume and effective porosity [23-27].

Fluctuations in groundwater elevation (GWE) can also lead to changes in hydraulic conductivity because as the water table rises or falls it may encounter layers with different hydraulic conductivity values. These fluctuations can cause changes in the hydraulic gradient that are associated with groundwater velocity and can result in changes in residence time and preferential groundwater flow [28, 29]. The hydraulic conductivity, local geochemistry of the groundwater, and mineralogy of the aquifer are important considerations when preparing a treatment plan [30]. Familiarity and analysis of these properties can increase the likelihood of an efficient and successful treatment. However, these properties have the potential to change once an amendment is applied and treatment progresses. The general direction of groundwater flow is determined during treatment design; however, preferential flow paths may change after an amendment is introduced and interacts with the aquifer media, groundwater, and the subsurface microbial community. To design more effective bioimmobilization treatment plans, these factors may need to be more carefully considered and better understood for success of the initial, and subsequent, injections.

This thesis aims to determine the impact of EVO amendments experimentally on hydraulic conductivity, along with the magnitude and significance of those impacts, in an aquifer with a history of uranium contamination and EVO exposure. If the injection of EVO causes changes in hydraulic conductivity, then a significant difference will exist between the injection wells, down-gradient monitoring wells, and the control well throughout the duration of the experiment post-injection. If these changes in hydraulic conductivity are related to the effectiveness of the biostimulation treatment, then there will be a difference in the reduction of

aqueous uranium concentration between the injection wells, down-gradient monitoring wells, and the control well.

CHAPTER TWO
LITERATURE REVIEW: CHANGES IN HYDRAULIC CONDUCTIVITY RELATED TO ELECTRON DONOR INJECTION

Changes in hydraulic conductivity can occur in an aquifer undergoing remedial action through many different processes. These include interactions of the amendment with aquifer media, water table fluctuations, dissolution/precipitation of minerals, fine particle release and capture, and bioclogging. However, some of these properties may be negligible given the magnitude of their effects within the time scales they occur. Ultimately, changes in hydraulic conductivity can result in inadequate dispersion of an amendment and cause changes in groundwater flow that can result in contaminated groundwater bypassing the area of injection.

Amendment Effects

Emulsified vegetable oil (EVO) amendments have been successfully used to stimulate microbial communities in aquifers to bioimmobilize uranium [2, 3, 31]. However, indefinite immobilization is unlikely because bioreduced uranium can be reoxidized by slight environmental perturbations that introduce oxygen or nitrate. Because of this, subsequent treatments, or alternative approaches, are needed to maintain the conditions for immobilization [32]. It has been observed that aquifers previously exposed to an amendment, or electron donor, will respond to and degrade the amendment more quickly on subsequent exposures [9, 11]. This phenomenon is referred to as the "memory effect." Although the memory effect is widely accepted, field observations of its occurrence in the context of amendment dispersion is lacking.

The radius of injection (ROI) of an EVO emulsion varies based on soil type, permeability, and heterogeneity [24]. ROIs of 2.1 – 3 meters have been observed in silty clay-

like soils, with ROIs up to 2.4 – >4.5 meters in sandy soils. Emulsions were observed to disperse at least 30 meters from the point of injection in sandy gravel mixes [24]. ROI is directly related to the hydraulic conductivity and freedom of the amendment to disperse once injected. In some instances, hydraulic conductivity may be more important overall than microbiology and chemistry for biostimulation to be successful at a particular site [30].

It is generally accepted that the aquifer should have an average minimum hydraulic conductivity of 10^{-4} cm/s for a site to be considered suitable for biostimulation (**Figure 2**) [33]. Initial site characterization may conclude that an area is suitable for biostimulation. However, in an area that is known to be highly heterogeneous, there can be significant spatial variation in the hydraulic conductivity that is related to the preferential flow of groundwater. Because of this, the volume of groundwater traveling through the subsurface can vary substantially depending on the location.

Furthermore, physical properties of an amendment, such as viscosity, specific gravity, and variations in droplet size, can lead to decreases in hydraulic conductivity once injected. An area once deemed suitable for amendment injection may have changes in these important properties once an amendment is introduced. This concept becomes more relevant as subsequent injections occur in the same area and the possibility of increased response and degradation due to the "memory effect." Previously, it has been shown that reductions in hydraulic conductivity can mostly be attributed to physical straining of droplets in pore constrictions smaller than the diameter of the droplet and by emulsion droplets adhering to pore walls [34]. Because emulsion droplets are typically much smaller than pore diameters, it seems more likely that the occurrence of droplets adhering to pore walls would play a greater role [35]. However, in an area with a

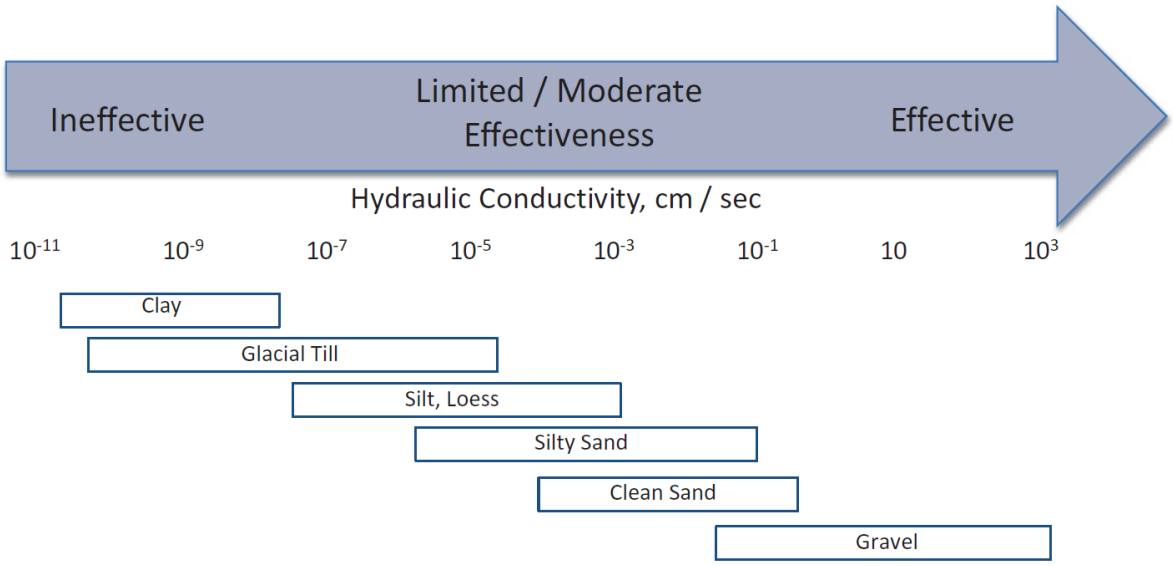


Figure 2. The effectiveness of biostimulation in relation to hydraulic conductivity (after Hazen, 2018 [6]).

highly heterogeneous subsurface, such as area of the aquifer used in this study, a greater range of pore constrictions can exist that may result in a limited freedom of movement, regardless of droplet size.

The mean droplet size within an emulsion can vary depending on the application for which it is being used. For example, Terra Systems, Inc. (Claymont, DE), produces an emulsion with a mean droplet size of 5 µm [micron] for maximum retention within areas of high groundwater flow. This company also produces a nonionic, small droplet size formulation, with a mean droplet size of 0.6 µm for use in aquifers that are composed of sand, silt, or clay. Choosing the correct droplet size for the application is nontrivial. An amendment composed of 0.6 µm droplets may be flushed through an aquifer with high groundwater flow before microbes begin to utilize it and deplete oxygen and nitrate present before reducing uranium. On the other hand, an amendment composed of 5 µm droplets injected within a sand, silt, or clay aquifer would likely fail to disperse adequately before being degraded close the point of injection. In either case, the effectiveness of the treatment can be reduced.

Modelling and lab-based studies have shown that changing the injection rate or dilution rate have little effect on the ability and extent that an EVO injection will disperse throughout an aquifer [5]. Ultimately, the amendment will mix with groundwater, which will disperse it throughout the site over time, or remain in residual concentrations, that may eventually be degraded. However, residual concentrations can have lasting effects on aquifer hydraulic conductivity. Significant differences in hydraulic conductivity resulting from residual EVO can alter preferential flow and may negatively impact the effectiveness of subsequent injections meant to maintain conditions necessary for bioimmobilization [13].

Even with optimal droplet sizes, as droplets of EVO disperse, they can collide and stick to aquifer surfaces [36]. EVO emulsions are known to be unstable and droplets may coalesce to form larger droplets over time [14]. Retention of these droplets is higher in proportion with clay content [13, 37]. Coulibaly and Borden [13] found that residual saturation was higher in material that was more broadly graded and heterogeneous. During their sand column experiments, the permeability after 20 pore-volumes (PV) of water displacement was reduced by slightly less than half of the initial value. They also observed reductions of hydraulic conductivity of 40% after the injection of a fine droplet EVO emulsion into a column which then recovered to pre-injection values. This loss of hydraulic conductivity was attributed to larger droplets being allowed to move through the substrate and eventually clog smaller pores. If these changes in hydraulic conductivity create a significant difference in hydraulic conductivity between the clogged area and the surrounding area, then groundwater can exhibit preferential flow towards areas of higher hydraulic conductivity. This will cause a large volume of groundwater to bypass the injected amendment and result in inadequate dispersion. Even if the treatment may eventually disperse over time, this still leaves the possibility of significant volumes of contaminated water bypassing the treatment zone. Furthermore, due to the increased retention time, much of an EVO amendment may be degraded at the point of injection before it eventually begins to disperse down-gradient. This can result in reduced response in down-gradient wells due to an inadequate volume of amendment reaching them.

At typical groundwater temperatures (10°C – 20°C), soybean oil has a viscosity that is 60 – 70 times that of water [13]. A viscosity of this magnitude can make moving an amendment down gradient more difficult. Low viscosity oil emulsions can result in permeability reductions

of up to 80% [38]. Increases in hydraulic gradient of up to two orders of magnitude have also been observed, which were attributed to the introduction of the amendment [13]. It was also found that once residual saturation levels were reached, after 20 PV, hydraulic conductivity returned to approximately half of the original value [13]. Biostimulation resulting in the immobilization of contaminants requires subsequent injections to maintain conditions and prevent reoxidation of bioimmobilized contaminants [2, 10]. In this context, the repeated injections may eventually result in the hydraulic conductivity within the treatment area decreasing to the point that biostimulation using EVO is no longer an effective method of treatment.

Water Table Fluctuations

Fluctuations in the water table can result in changes in the hydraulic conductivity within an area. It has been shown that saturated hydraulic conductivity generally decreases with depth and can influence groundwater flow, velocity, preferential flow paths, and the residence time associated with these flow paths [28, 29]. As depth increases, the weight of the overburden, and related compressive forces, increase, which can result in a reduction in the available volume within pore space and fractures. As GWE decreases the water table can be at depths where hydraulic conductivity is likely to be less than when nearer to the surface. Furthermore, layers within an aquifer can differ greatly in their composition and have a non-trivial difference in their hydraulic conductivity values. If GWE surpasses the boundary between layers, then the movement of groundwater will be limited by the hydraulic conductivity within that layer. Should GWE change such that the water table exists in two different layers, groundwater flow will be impacted by the interactions between the two differing layers.

Fluctuations in GWE can also result in changes to the hydraulic gradient [39]. The hydraulic gradient is calculated by measuring the hydraulic head at two points and the distance between those points, then applying the following equation [39],

$$I = \frac{dh}{dl} = \frac{h_2 - h_1}{\text{length}}$$

Where:

I = Horizontal hydraulic gradient [dimensionless]

dh = the difference between two hydraulic heads [L]

dl = the flow path length between the two hydraulic head measurements [L]

The horizontal hydraulic gradient (*I*) is related to hydraulic conductivity (*K*) and the average linear velocity of groundwater (*V*) through the following equation.

$$V = \frac{KI}{n}$$

Where:

V = Average linear groundwater velocity [L/t]

K = Hydraulic conductivity [L/t]

I = Horizontal hydraulic gradient [dimensionless]

n = Effective porosity [dimensionless]

In an aquifer with large variations in hydraulic conductivity, groundwater velocity can be very sensitive to changes in GWE and the associated hydraulic gradient. These properties can impact the volume of groundwater flowing through and area and the residence time of the groundwater. Assuming effective porosity and hydraulic conductivity remain unchanged, an

increase in the hydraulic gradient will result in an increase of the groundwater velocity. Similarly, a decrease in the hydraulic gradient will result in a decrease in groundwater velocity. Assuming effective porosity remains unchanged, it is also possible that a decrease in hydraulic conductivity and an increase in hydraulic gradient, or vice versa, could change in such a way that groundwater velocity is unchanged.

Mineral Precipitation, and Dissolution

Mineral precipitates are common products of changes in groundwater geochemistry in the subsurface. Once a significant degree of super-saturation for a mineral phase is reached, mineral phases may precipitate through nucleation or crystal growth. Precipitation of minerals can then lead to reductions in porosity and permeability as available pore space is reduced [16, 25, 40]. This occurs either through coating the inside surfaces of pores and fractures, plugging of pore throats, or a combination of the two. In previous studies, models have shown a decrease in porosity and permeability due to mineral precipitation [17, 41]. These same modelling studies have also shown an increase in these same properties due to dissolution. Precipitates have been shown to manifest as sulfate scales and other amorphous mineral phases, which are more thermodynamically driven, following the mixing of formation water and injection water. Precipitating crystals can also be attracted to pore surfaces through attractive forces. This also leads to a reduction in available volume within the pore and may also block a pore throat entirely and leads to reductions in hydraulic conductivity, permeability, and effective porosity. In attempts to bioimmobilize U(VI), it is reduced to insoluble U(IV) to reduce mobility in the aquifer.

Fines and Colloids

Formation water is typically gathered and mixed with emulsified vegetable oil before the amendment is applied. This process can release fines and colloidal particles that are then reintroduced to the aquifer that can lead to reduced pore volume and effective porosity [23, 26]. Both aquifer properties can ultimately affect the hydraulic conductivity of the treatment area. Fines can adhere to pore walls through attractive forces and obstruct pore throats that can reduce permeability and effective porosity [25]. During undisturbed groundwater conditions, colloids are typically immobile[26]. Deviations from native groundwater conditions, such as injection of water with a different chemical composition or varying flow rates, can lead to colloids being released, transported, and redeposited down gradient [25, 26]. It should be noted that there is little agreement regarding the effects of flow velocity on colloid release [26]. Observations in previous studies have ranged from showing small releases of colloids with an increase of flow velocity to indications that colloid release greatly depends on this factor [26]. There are also conflicting reports regarding the response time of colloids to flow velocity with studies showing a rapid response and release to increased flow velocity versus slow response and release to an increase in flow velocity [26]. Even when colloids are much smaller than pore throats, hydrodynamic bridging can occur when multiple colloids simultaneously arrive at a pore throat and block it completely [27]. Release of colloids can also occur due to changes in ionic strength (IS). The results from Torkzaban et al. [26] state that they agree with previous studies and show that a decrease in IS induced colloid release because of its effect on colloid-colloid and colloid-collector interaction energies. Torkzaban et al. [26] also observe permeability decreases in cores

that were at least 6.1% to 7.4% kaolinite. They attribute this decrease to hydrodynamic bridging that occurred when IS was decreased and colloids were released.

Bioclogging and Microbial Effects

Bioclogging can also occur due to growth of bacteria and result from the increased availability of nutrients and carbon sources from an EVO injection. Biofilms form on fracture networks and cause reduced effective porosity [18, 19, 25]. Sulfate-reducing bacteria (SRB) are specifically mentioned and are also significant in the context of bioremediation [19]. Taylor et al. [18] also mention that under anaerobic conditions, which are required for many biostimulation techniques, biogases produced by microbes can accumulate and block pores, which leads to reductions in permeability. Studies have shown that bacterial growth results in a reduction of permeability in sandstone cores due to biofilm production [20]. Near the screened interval of the injection well, bacteria attach to available surfaces and produce thick biofilms composed of exopolysaccharide slime. In a model core experiment, a reduction in permeability was observed and attributed to the occurrence of biofilms [19]. Taylor et al. [18] created a model to describe the effects of microbial biofilms on permeability. However, the model assumes that the biofilm would be a uniform thickness. They mention this shortcoming in their study and make note of the variability of physical, chemical, and biological processes that occur a natural environment and ultimately they suggest that biofilm thickness would be better described as a random variable [18]. Another investigation into bioclogging used a single-fractured section of limestone and measured the change in hydraulic conductivity once the microbial population was stimulated [21]. After eight days, hydraulic conductivity decreased to 86% of its original value prior to stimulation. After 22 days, the hydraulic conductivity within the single-fracture was reduced to

0.8% of the initial hydraulic conductivity. Although biofilms may lead to slight reductions in effective porosity, their presence is difficult to measure in-situ. However, efforts to model the reductions in porosity and hydraulic conductivity related to biofilm formation have been validated with experimental data from column experiments with errors in predicting porosity below 3% and hydraulic conductivity below 10% [22].

Although all of the factors discussed within this chapter may occur to some degree, studies indicate that the processes most likely to cause the most significant changes in hydraulic conductivity are clogging due to pore blockage by EVO droplets. In the time scales within which these amendments are planned to be effective, other factors, like mineral precipitation and dissolution, will likely be minimal when compared to the more direct effects of the amendment itself.

CHAPTER THREE
SITE BACKGROUND, GOALS, OBJECTIVES, AND HYPOTHESES

Site Background

The site used in this study is within a shallow, unconfined aquifer located in Area 2 of the Oak Ridge Field Research Center (ORFRC) inside of the Y-12 National Security Complex, located in Oak Ridge, Tennessee. The Area 2 site is part of a shallow gravel pathway created to facilitate the migration of uranium contaminated groundwater to seeps in the upper reach of Bear Creek [42]. The upper 6 m of the subsurface is composed of an unconsolidated and heterogeneous mix of gravel consisting of Maynardville Limestone, along with silty and clayey fill derived from decomposed shale and limestone (**Figure 3**) [2, 10, 11, 43-45]. Below the fill lies undisturbed clay-rich weathered saprolite that can have hydraulic conductivities at least two orders of magnitude less ($4.1x10^{-5}$ cm/s) than the overlying fill ($3.8x10^{-2}$ cm/s) [2, 42-44, 46]. Undisturbed saprolite within ORNL has been shown to retain bedding features and fractures along with numerous macropores formed from plant roots and soil fauna [47]. It is unknown if these features are present in the reworked gravel and saprolite fill which is present in Area 2. Previous shallow subsurface measurements have reported geometric means of $9.61x10^{-3}$ and $1.97x10^{-4}$ cm/s within this subcatchment [48]. These measurements are an order of magnitude less than what has previously been measured at this particular site. However, since Area 2 has been excavated, reworked with gravel, and filled, large differences are to be expected. Reported values for hydraulic conductivity from various studies within Area 2 and nearby areas with similar geology can be found in **Table 1**.

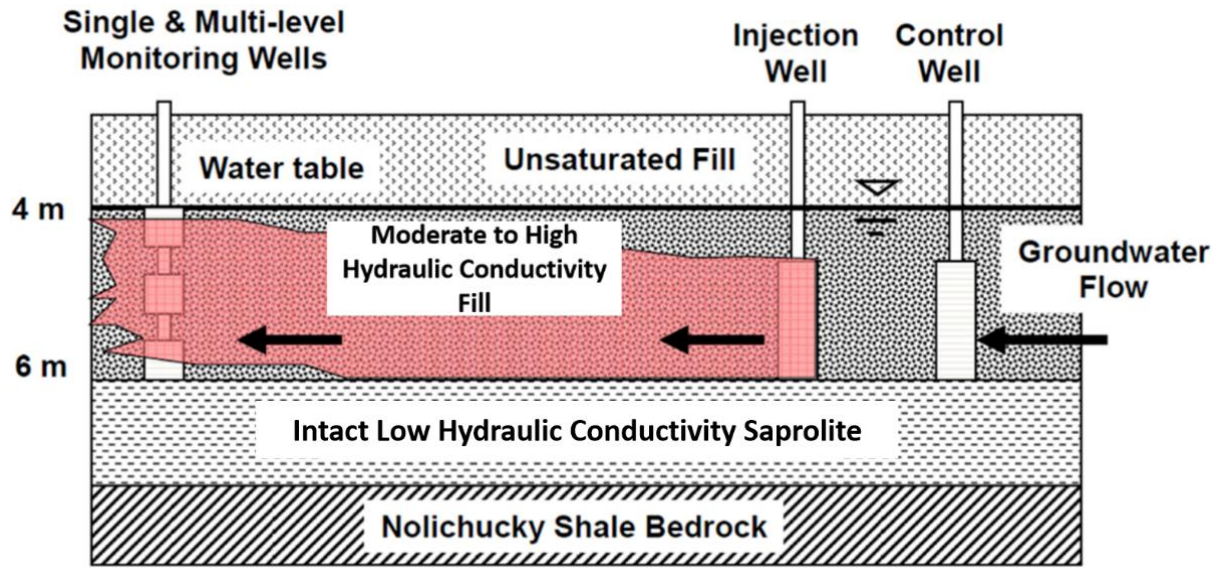


Figure 3. A cross-section representative of the Area 2 sub-surface, not to scale (modified from Watson et al., 2013 [2]).

Table 1. Reported values for hydraulic conductivity (cm/s) in Area 2 and other sites in Bear Creek Valley with similar geology. Locations other than Area 2 consist of wells screened in intact saprolite or regolith overlying it rather than the reworked saprolite and gravel fill present in Area 2. Bedrock refers to the underlying Nolichucky Shale [2, 11, 42, 43, 48-50].

Location	**Hydraulic Conductivity (cm/s)**		**Source**
	Saprolite/Fill	Bedrock	
Area 2	$2.1x10^{-4}$ to $1.6x10^{-3}$	10^{-8}	Paradis et al. (2017) [41]
Area 2	$6.9x10^{-4}$ to $1.8x10^{-3}$	NA	Paradis et al. (2018) [11]
Area 2	$1x10^{-2}$	10^{-9} to 10^{-4}	Watson et al. (2004) [44]
Area 2	$3.8x10^{-2}$	$4.1x10^{-5}$	Watson et al. (2013) [2]
Bear Creek Valley (various locations)	$1.31x10^{-5}$ to $1.1x10^{-3}$	$1.62x10^{-7}$ to $2.36x10^{-3}$	Connell and Bailey (1989) [47]
SWSA-7	$1.97x10^{-4}$ to $9.61x10^{-3}$	NA	Wilson, Aflonis, and Jardine (1989) [46]
Burial Grounds 5 & 6	$2.36x10^{-3}$ to $7.76x10^{-5}$	NA	Webster and Bradley (1988) [48]

In 1951, four unlined impoundments with the dimensions of 122-m x 122-m and 5.2-m in depth, known as the S-3 waste disposal ponds, were constructed to hold liquid nitric acid and uranium-bearing wastes [42]. Until 1983, waste was transported to these ponds via a pipeline at the rate of approximately 10 million liters/year. The stored waste began to infiltrate and contaminate groundwater in the surrounding area [51]. Biodenitrification and neutralization of the S-3 ponds was attempted in 1984. In 1988, the S-3 ponds were closed, neutralized, back-filled, and capped with asphalt to reduce infiltration from precipitation. The former S-3 ponds now exist as a parking lot (**Figures 4 & 5**). Nitrate concentrations near the source zone have been reported as high as 11,000 mg/L [52], which has caused significant issues with attempts to bioimmobilize and bioneutralize contaminants near the source. The Area 2 site used in this study is approximately 300-m south of the former S-3 waste disposal ponds.

This site and subset of wells (**Figure 6**) have been used in previous studies, most recently in 2009 [3], which used EVO injection as a method of biostimulation to reduce dissolved uranium concentrations [2, 3, 31, 32, 46]. However, these studies focused on the geochemistry and microbiology and did not monitor changes in hydraulic conductivity that may have occurred once an amendment was introduced. There are three injection wells, four down-gradient monitoring wells, and one up-gradient control well located at the site used within Area 2. Previous studies used bromide as an inert tracer to confirm that these wells were interconnected [2, 3]. A previous study within Area 2, although with a different subset of wells, was recently conducted in an effort to improve the in situ estimation of effective porosity [43]. The effective porosity determined from the wells used in this study were found to range from a low of 0.6% to a high of 5.0%. Because this unconfined aquifer has such low effective porosity, it is likely to be

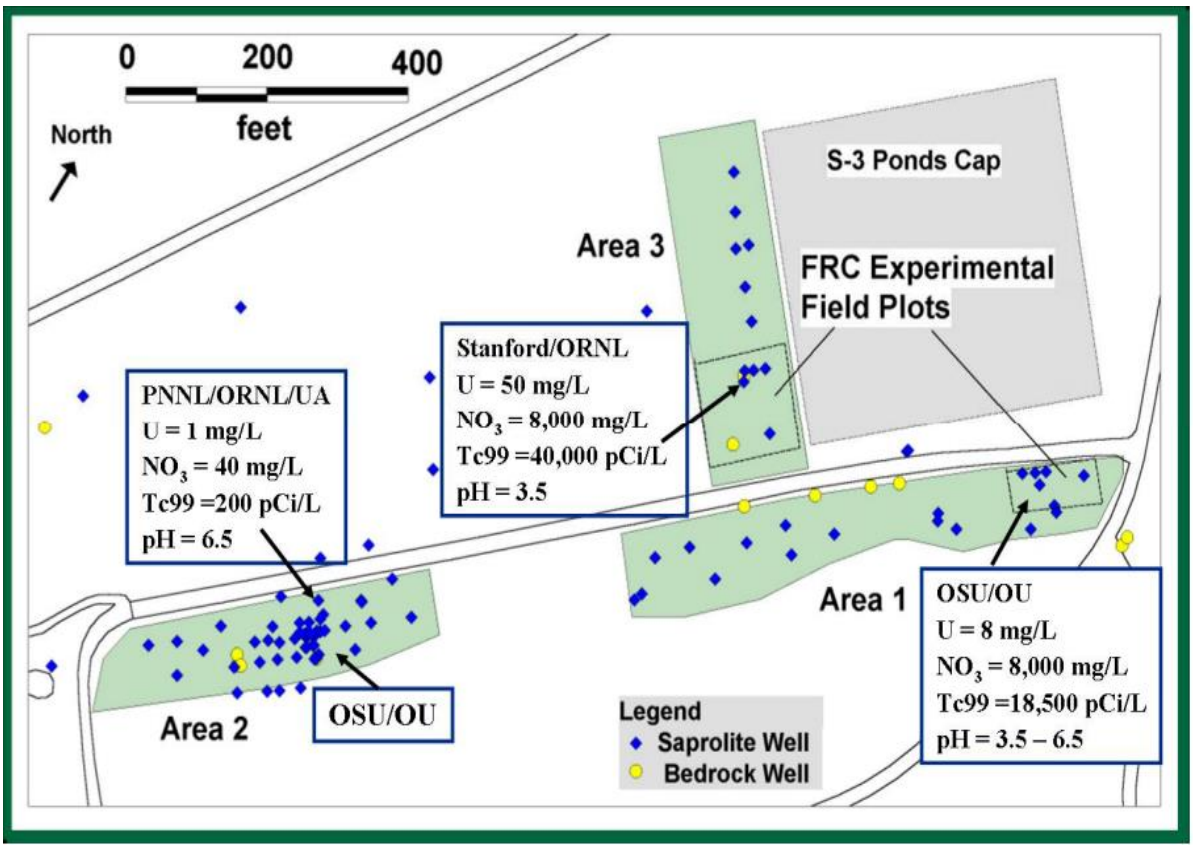


Figure 4. The Oak Ridge Field Research Center with typical groundwater quality and contamination levels for the areas around the former S-3 Ponds. The former S-3 Ponds are approximately 750 ft. (229 m) NE of the study site within Area 2. Wells labelled as “Saprolite Well” can be screened in either unconsolidated clay-rich fill or intact saprolite [42].

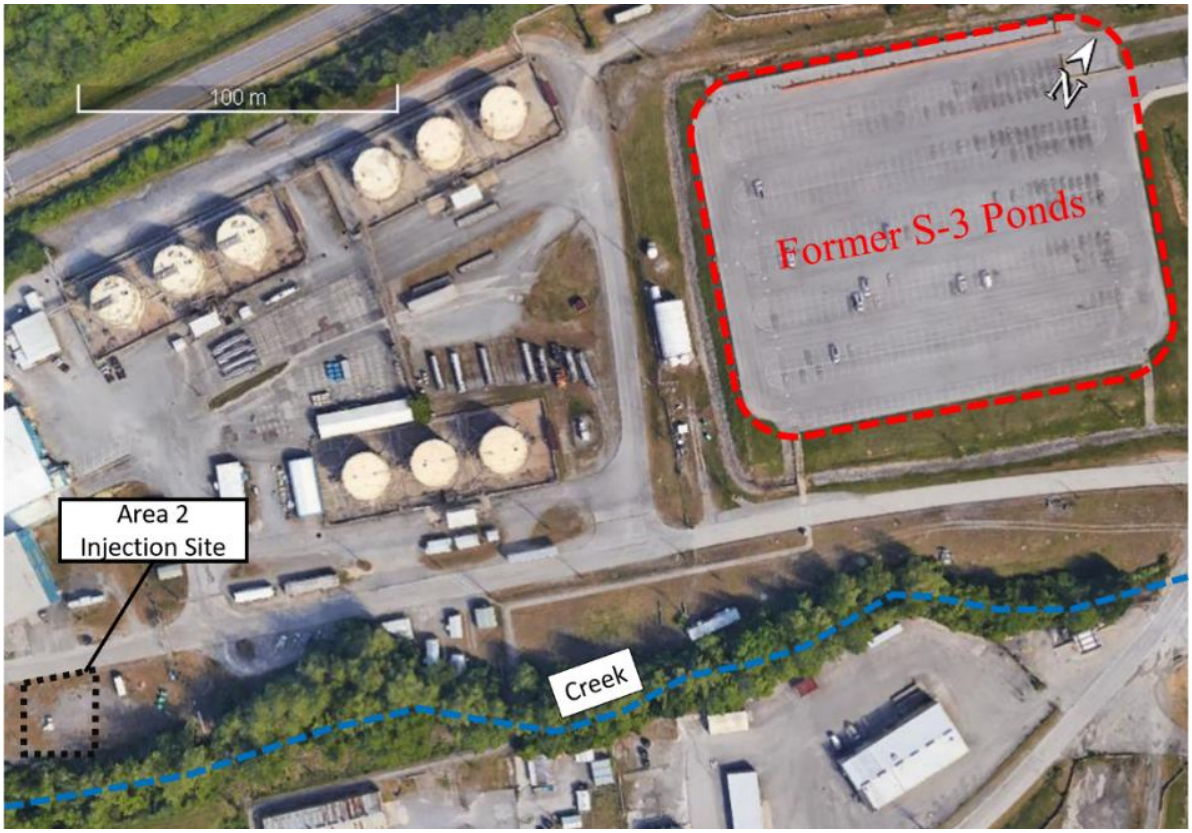


Figure 5. Annotated Google Earth imagery of the former S-3 Ponds and the injection site. (Edited from Google Earth Pro 7.1.8.3036 (32-bit) (April 12, 2018). Oak Ridge, TN. 35°58’37.74” N, 84°16’24.48” W, Eye alt 643m. http://www.earth.google.com [September 26, 2018]).

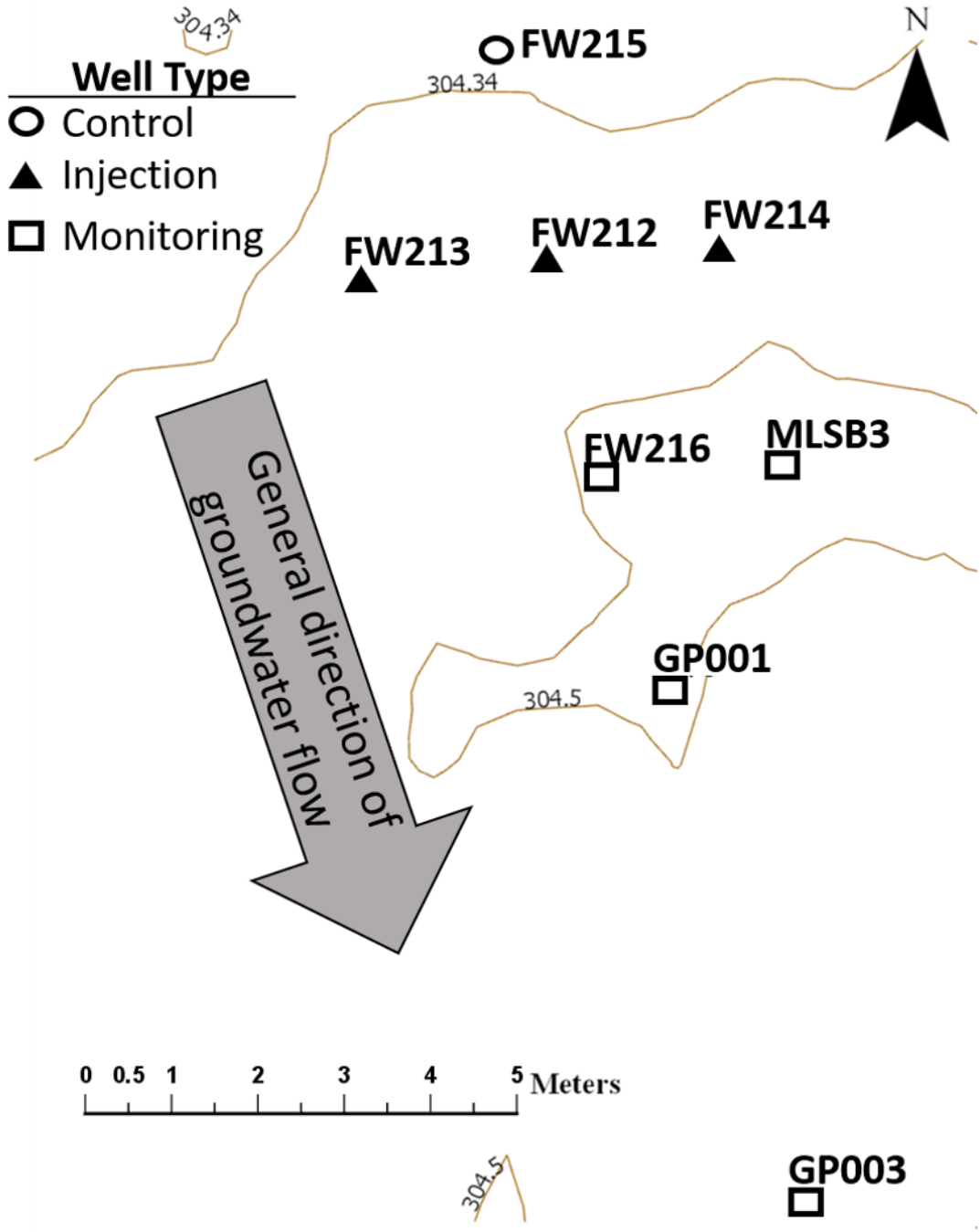


Figure 6. Plan view map of the injection site. Surface contours are brown and labeled in units of meters above mean sea-level (mamsl).

very sensitive to an EVO injection, making this an excellent site to observe the changes in hydraulic conductivity.

Goals

This study was conducted with two other researchers focusing on different aspects related to the experiment, specifically the "memory effect" of the microbial communities previously exposed to EVO and the role of different sizes of bacteria [53]. The portion of the experiment addressed within this thesis focuses on the changes in hydraulic conductivity related to the injection of EVO and the effectiveness of the amendment in reducing dissolved uranium concentration in a previously treated aquifer. The main goal of this thesis is to observe the post-EVO injection change in hydraulic conductivity in down-gradient wells, the injection wells, and the control well. A secondary goal is to determine if changes in hydraulic conductivity correlate to changes in dissolved uranium present in the groundwater.

Objectives and Hypothesis

The specific objectives are to:

1. Measure the changes in hydraulic conductivity over time after an injection of EVO.
2. Measure changes in dissolved uranium and associated aquifer geochemistry and compare those to changes in hydraulic conductivity and hydraulic gradient over time after an injection of EVO.
3. Determine if statistically significant differences exist in hydraulic conductivity and dissolved uranium between wells and between well type (control, injection, monitoring) over time.

4. Determine if a statistically significant correlation exists between hydraulic conductivity, dissolved uranium concentrations and associated geochemistry.

5. Determine if degradation of EVO, indicated by acetate generation, happened faster in this injection than during the most recent 2009 injection at the same site.

The specific hypotheses to be tested are applicable to changes observed over the course of the experiment and include:

i. H_1: The hydraulic conductivity in the injection and down-gradient monitoring wells is lower after EVO injection.

   H_0: There is no difference between pre-injection and post-injection hydraulic conductivity values in the injection and down-gradient monitoring wells.

ii. H_1: The hydraulic conductivity in the control well is not lower after EVO injection.

   H_0: The hydraulic conductivity in the control well is lower after EVO injection.

iii. H_1: The dissolved uranium concentrations in the injection and down-gradient monitoring wells are lower after EVO injection.

   H_0: There is no difference between pre-injection and post-injection dissolved uranium concentrations in the injection and down-gradient monitoring wells.

iv. H_1: Dissolved uranium concentrations in the injection and down-gradient monitoring wells are lower than in the up-gradient control well after EVO injection.

   H_0: Dissolved uranium concentrations in the injection and down-gradient monitoring wells decrease relative to the up-gradient control well after EVO injection.

v. H_1: Hydraulic conductivity affects the concentrations of dissolved uranium after EVO injection.

H_0: Hydraulic conductivity does not affect the concentrations of dissolved uranium after EVO injection.

vi. H_1: Acetate generation occurs earlier than in the 2009 injection, suggesting a memory response to EVO.

H_0: Acetate generation did not occur earlier than in the 2009 injection, suggesting that there is no memory response to EVO.

CHAPTER FOUR
MATERIALS AND METHODS

Summary of Injection and Sampling Schedule

Groundwater sampling and hydraulic conductivity measurements began on December 7, 2017, 6 days before the EVO injection. Once arriving on site, all wells had their groundwater elevation measurements recorded before any pumping or sampling occurred. This was followed by a steady-state drawdown pumping test to acquire the data used to calculate hydraulic conductivity. Once the initial steady-state drawdown measurements were completed, groundwater samples were then collected for biogeochemical analysis while monitoring drawdown until sampling was completed. This process was completed in all wells, except for the injection wells, which were only sampled for geochemistry and not microbial analysis. Precipitation data from for the study period was acquired from Y-12 Meteorology services. Measurements were taken from the West Tower, which is located approximately 560 m north of Area 2.

The EVO injection occurred December 13, 2017 (Day 0). No samples were collected for analysis on this day. Sampling resumed the next day, December 14, 2017 (Day 1), and continued weekly for 3 weeks. After the first 4 weeks of sampling, the time interval between samples was increased to once a month. Monthly sampling continued until April 26, 2018, which was 134 days after the EVO injection (**Table 2**).

Table 2. An outline of the field work schedule followed during the experiment.

Date	Days Since Injection	Type
December 7, 2017	-6	Background
December 13, 2017	0	Injection
December 14, 2017	1	Weekly
December 21, 2017	8	Weekly
December 28, 2017	15	Weekly
January 4, 2018	22	Weekly
February 1, 2018	50	Monthly
March 1, 2018	78	Monthly
March 29, 2018	106	Monthly
April 26, 2018	134	Monthly

Well Inspection and Preparation

The control well (FW215) and the three injection wells (FW212, FW213, FW214) are constructed of 4.32-cm (inside diameter) schedule 40 polyvinyl chloride (PVC) pipe. Monitoring well FW216 was constructed of 1.88-cm (inside diameter) schedule 40 PVC pipe. Monitoring well MLSB3 was part of a 7-port multiport well (MLSB), which used a 4.32-cm inside diameter Solinst® CMT 7-channel system (Georgetown, Ontario, CA) [54]. The third port (MLSB3) was screened within the same level as other wells used in the study. Monitoring wells GP001 and

GP003 were screened within two intervals and were constructed of 5.2-cm (inside diameter) schedule 40 PVC pipe with a smaller, 1.88-cm (inside diameter) schedule 40 PVC pipe nested inside with a packer separating the well into two screened intervals. The construction of the monitoring wells prevented the use of down-well devices, such as a borehole camera, data-logging pressure transducer, or bailer. Well casings of the control and injections wells were visually inspected using a Well-Vu (Brainerd, MN) well inspection camera system (Model WV-300FEDV) to verify the integrity of the well casing and screened area. The wells looked to be in excellent condition structurally with some biofilm present on the inner walls of the casings. None of the monitoring wells were able to have the inside of their well casings inspected because the inner diameter of their well casings are less than the diameter of the borehole camera. The surge block method was used to release fines and biofilm on the well screen of the injection wells and reduce the likelihood of blockages near the well casing. A PVC surge block was inserted into the well casing, starting above the screened interval, and repeatedly raised up and down, approximately 0.5 – 1 m, at around 30 strokes per minute. This process was repeated until the entire screened interval had been developed [55].

Emulsified Vegetable Oil (EVO) Source and Composition

The EVO was purchased from Terra Systems, Inc. (Claymont, DE). The composition is slightly different than what was used in the 2009 study [3] due to the older formulation no longer being produced by the manufacturer. The EVO used in this study did not include yeast extract or $(NH_4)_3PO_4$ [ammonium phosphate], but did include lactate. Lactate and polylactate compounds have been shown to effectively stimulate microbial communities to bioimmobilize metals [56]. A total of 208.2 L of EVO was procured in eleven 18.93-liter plastic buckets with sealed lids. The composition of the EVO can be found in **Table 3**.

Table 3. Composition of EVO solution used for injection.

Ingredient	wt. %
Food grade soybean oil	60
Food grade sodium or potassium lactate	4
Proprietary food grade nutrients	<1
Proprietary food grade emulsifiers and preservatives	7.5
Vitamin B12	<1
pH	6.5 - 7
Median oil droplet size	0.6 μm

EVO Preparation and Injection

On the morning of December 13, 2017, approximately 833 L [liters] of groundwater was simultaneously pumped from the three injection wells (FW212, FW213, FW214) into a 1,987-liter container using three peristaltic pumps. Each pump extracted groundwater at the rate of 2.8

L/min [liters per minute], resulting in a total of 8.4 L/min with all three pumps running simultaneously. Once the groundwater was extracted, the EVO was added, one 18.93-liter bucket at a time, to create 1041 L of colloidal suspension containing 20% EVO and 80% native groundwater. This is less than what was used in the 2009 by Gihring et al. [3] during their injection experiment at this same site. They injected approximately 3,400 L of EVO-groundwater emulsion. Due to the large volume that was injected in 2009, the amendment travelled upgradient and contaminated the control well. To avoid this previous problem, the volume required was recalculated using the lower bound of estimated porosity within the study area.

Once all of the EVO was added to the container, both the inlet and outlet of the tubing used in the peristaltic pump were placed into the container to thoroughly mix the groundwater and EVO by circulating the contents for 45 minutes. Once mixing was completed, the outlet tubing was inserted into the injection wells. The EVO and groundwater mixture was then injected into the three injection wells simultaneously at the rate of 2.8 L/min, for a total rate of 8.4 L/min, until the container was empty. Flushing was not done after injection in the previous experiments at this site [2, 3], so it was not done in this experiment either.

Measuring Hydraulic Conductivity

Because none of the monitoring wells could accommodate a down-well device or a bailer for conducting slug tests to determine hydraulic conductivity, a different method was chosen that used well construction data and low-flow pumping data. Robbins et al. [57] determined that results are statistically equivalent to slug tests. Aragon-Jose & Robbins [58] used this method to test five wells at three different pumping rates and drawdown measurements. Their results showed that this method provides consistent results in groundwater wells, even when pumping

rates and their associated drawdown differ. It has also been successfully used at this same site in a previous study with a different subset of wells [43]. Robbins et al. [57] determined that this method is practical in that it can be used to achieve steady-state drawdown at a high enough pumping rate to minimize duration of sampling in aquifers with hydraulic conductivities greater than 10^{-6} cm/s. They also note that accurately measuring drawdown can be difficult at the typical U.S. EPA [59, 60] regulatory mandated maximum sampling rate of 1 L-min or less in high hydraulic conductivity constrained environments. Robbins et al. [57] calculated a practical upper conductivity limit for this method using the maximum pumping rate of 1 L/min and typical accuracy of water level meters (0.6 cm) and pressure transducers, resulting in an upper limit of 10^{-3} to 10^{-2} cm/s. The water level meter used to measure drawdown in this experiment is marked at 1 ft (30.48 cm), $1/10^{th}$ ft (3.048 cm), and $1/100^{th}$ ft (0.3048 cm), or an accuracy of 0.01 feet (0.3048 cm) as recommended by the U.S EPA [59, 60]. When considering the minimum measurable interval using this water level tape, 0.3 cm, at the maximum pumping rate of 1 L/min the upper limit of conductivity is 10^{-1} cm/s. Along with being a time efficient method, it has the added benefit of providing hydraulic conductivity values that are indicative of the conditions during sampling. Since the well screen is fully submerged within the saturated zone, the full ellipsoid Hvorslev equation was used to determine values for hydraulic conductivity once data were acquired [57].

First, static depth to water measurement was taken using a water level interface meter/measuring tape (Solinst) with markings every 0.3 cm. Next, the well was pumped using a peristaltic pump and depth to water was monitored. If no drawdown was observed, then the pumping rate was increased (≤1 L/min) until drawdown was observed and maintained a steady

state. Pumping rate was then determined by measuring the discharge of the groundwater into a graduated container for two minutes. Drawdown was then monitored while 10-liters of groundwater were recovered for microbial analysis in a separate study [53]. The pumping rate at steady state, change in groundwater elevation, and well construction data were used as inputs into a modified version of the Hvorslev equation to calculate hydraulic conductivity [57],

$$Q = \frac{2\pi LKH}{2.303log\left[\frac{L}{D} + \sqrt{1 + \left(\frac{L}{D}\right)^2}\right]}$$

Where:

Q = Steady state flow rate [V/t]

H = Steady state drawdown [L]

L = Length of screened interval [L]

D = Internal diameter of well casing [L]

K = Hydraulic conductivity [L/t]

Which can be rearranged to:

$$K = \frac{2.303log\left[\frac{L}{D} + \sqrt{1 + \left(\frac{L}{D}\right)^2}\right]}{2\pi LKH} Q$$

Well construction data used to calculate hydraulic conductivity can be found in **Table 4**.

Table 4. Well construction data used to calculate hydraulic conductivity.

Well ID	Diameter of well casing (cm)	Length of screened interval (meters)	Beginning of screened interval (mbgs)	End of screened interval (mbgs)
FW212	4.32	1.46	4.55	6.01
FW213	4.32	1.46	4.24	5.70
FW214	4.32	1.46	4.29	5.75
FW215	4.32	1.46	4.21	5.67
FW216	1.88	0.58	4.09	4.67
MLSB3	4.32	0.08	4.90	4.98
GP001	5.2	2.89	2.56	5.46
GP003	5.2	2.87	2.82	5.69

Sampling Method

After pumping data was acquired to determine hydraulic conductivity, the sample tubing was connected to an *In-Situ* TROLL 9500 (Fort Collins, CO) with an attached flow-through cell and groundwater parameters were monitored until stable conditions were reached (temperature, pH, oxidation reduction potential (ORP), and conductivity). Once groundwater parameters stabilized, unfiltered samples were collected in 50-mL [milliliter] Falcon tubes. Samples were then stored in coolers with ice packs until sampling was completed. Groundwater was then filtered in the laboratory through polycarbonate (PCTE) 10-µm and nylon 0.2-µm filters. Two 20-mL sterile scintillation vials were then filled, with no headspace, from each well and each time point. One vial to be used for cation analysis was acidified with 100 µL of 1M HCl and stored at 4°C. The second vial was stored at 4°C for anion analysis.

HPIC and ICP-MS Sample Analysis

Organic acids and anion concentrations were determined with a DionexTM ICS-5000+ series high pressure ion chromatography (HPIC) system using an AS11-HC column at 35°C with potassium hydroxide (KOH) eluent. Chromeleon (ThermoFisher Scientific, Inc., Waltham, MA) software and five internal standards were used to calculate calibration curves. Manual curves based on R^2 equations were used to produce curve values.

Cations and trace metal concentrations were measured by inductively coupled plasma mass spectrometry (ICP-MS) with an ELAN 6100 system (PerkinElmer, Inc. Waltham, MA) and a previously described method [61]. Samples were analyzed for concentrations of sodium, magnesium, aluminum, potassium, calcium, scandium, iron, manganese, terbium, and uranium. Prior to analysis, an internal standard covering the analytes was added to each sample. They

were then diluted with a 1% nitric acid solution and injected with the system's autosampler. Sample duplicates were run every 20 samples and calibration standards were run every 10 samples for quality control purposes. Although samples were preserved with HCl and diluted with nitric acid, they have not been known to cause interferences with these analytes before [62].

Some samples had significant amounts of visible EVO even after being filtered through 10-µm and 0.2-µm pore diameter filters. These were filtered through a 0.2-µm pore diameter filter again using a syringe filter. Samples that still appeared to contain visible EVO were then diluted to prevent interference with the column. Samples that required excessive dilution were not analyzed due to the likelihood of inaccuracies in the reported results.

Statistical Analysis

Statistical analysis was completed using the *Analysis Toolpak* in *Microsoft Excel* (2010) and *RStudio* [63, 64]. First, values were tested for normality using Q-Q plots and Shapiro-Wilks tests. For non-normal data, the 'Tukey Ladder of Powers' function in the *rcompanion* package was used to determine the best transformation to bring data to, or near, a normal distribution before continuing [65].

Next, a one-sample t-test was used to compare values in the control well to determine if a significant difference ($p < 0.05$) existed between pre-injection and post-injection values [66]. The results of this test were used to determine if the control well represented a well that was not contaminated or impacted by the EVO injection, in which case, it could be used as a true control. If data followed a normal distribution, then the raw data were used for this test. If the data were not normally distributed, then the transformed data produced by the 'Tukey Ladder of Powers' function from the *rcompanion* package was used [65]. Since there was only one pre-injection

measurement, that value was used as the hypothesized mean in the one-sample t-test. If the test reported that there was no significant difference ($p \geq 0.05$) between the pre-injection and post-injection values, this would suggest that the control well was not impacted by the EVO injection. If a significant difference ($p < 0.05$) was reported for hydraulic conductivity, whether this was related to an increasing or decreasing trend, then the control well could not be used as a true control. However, a significant difference reported for dissolved uranium concentrations was inspected to determine the nature of this difference. A trend of decreasing dissolved uranium concentrations would indicate that the control well was likely contaminated by the EVO injection and cannot be used as a control for statistical tests. A trend of increasing dissolved uranium concentrations would indicate that the difference is unlikely to be related to bioimmobilization of uranium and the control well was likely not contaminated by the EVO injection. If the control well was found to be unimpacted and uncontaminated by the EVO injection, then it was used as a control to test the other wells used in the experiment.

The control well was then compared to individual wells using a paired t-test [67]. The control well represents a well with no significant difference between pre-injection and post-injection values of hydraulic conductivity and was not impacted by the EVO injection. Results from this test would indicate if a well was impacted by the EVO injection and had significant differences between pre-injection and post-injection values of hydraulic conductivity and dissolved uranium concentrations. Since significant spatial variation exists in the values being tested, especially regarding hydraulic conductivity, the data in from all wells were normalized. This was done by taking the difference between the value for that sample and the pre-injection value then dividing that difference by the pre-injection value as shown,

$$x' = \frac{x_n - x_p}{x_p}$$

Where:

x' = normalized value

x_p = pre-injection value

x_n = sample value at day n

This results in all normalized pre-injection values being equal to zero and all normalized post-injection values being equal to the ratio between that value and the pre-injection value. This allows the magnitude of change relative to the pre-injection values to be compared and removes the influence of spatial variation. Once the data were normalized, a paired t-test was then used to compare the normalized post-injection hydraulic conductivity values of the individual injection and monitoring wells to the control well [67]. Pre-injection values were not included in this test since all wells had their values set to zero by normalization and all post-injection values represent the magnitude of difference relative to the pre-injection value after normalization. If no significant difference was reported, then the well compared to the control well had no significant difference between its pre-injection and post-injection values. If a significant difference was reported by the test, then the normalized data were inspected to determine if the difference was related to increasing or decreasing trends before the results were interpreted.

After testing individual wells against the control, they were then grouped into well types as injection, monitoring, or control to determine if a significant difference existed between those groups. Data that were normally distributed, or able to be transformed to a normality using 'Tukey's Ladder of Powers' test, were compared using a one-way ANOVA with well type as the

factor [65]. Data that were not normally distributed after transformation were tested using a non-parametric Kruskal-Wallis rank sum test with their untransformed values [63, 68]. Box and whisker plots were then used to help interpret the results of the one-way ANOVA or Kruskal-Wallis tests and identify the nature of the differences, or lack of difference, between well types. Results from this test would help determine if significant differences existed based on well type and if that difference is related to being injected with EVO.

Correlations were computed and the corresponding matrix was created using the 'sjt.corr' function from the *sjstats* package in *RStudio* [64, 69]. Because hydraulic conductivity was not normally distributed, the non-parametric Kendall correlation method was used with pair-wise deletion to determine the relationships that existed between completed pairs [70]. Cohen's d standard was used to evaluate the correlation coefficient and to determine the effect size and strength of the relationship [71]. A correlation coefficient between 0.10 and 0.29 represents a small relationship, whereas correlation coefficient between 0.30 and 0.49 represents a medium relationship, and a correlation coefficient of ≥ 0.50 represents a large relationship [71]. The correlation between hydraulic conductivity and dissolved uranium can be used to interpret the relationship between hydraulic conductivity and the effectiveness of the treatment in the vicinity of that well. A correlation between hydraulic conductivity and dissolved uranium would be expected if a significant amount of amendment were present, which can result in a reduction of hydraulic conductivity, and a corresponding reduction in dissolved uranium could be interpreted as resulting from bioreduction in this context. If it appears that bioreduction and immobilization of dissolved uranium are successful near a particular well, then it is expected that the dissolved uranium concentrations would be greatly decreased.

CHAPTER FIVE
RESULTS AND DISCUSSION

Groundwater Elevation (GWE)

Groundwater elevation values measured in meters above mean sea level (mamsl) and precipitation (cm) were measured during the 134 day period of the test. The purpose was to determine if there were any changes in GWE and assess whether they were likely caused by precipitation or by the EVO injection.

Pre-injection and post-injection GWE values for all wells are shown in **Figure 7**. Groundwater elevation values in all of the wells were between 300.42 and 300.48 meters above mean sea level (mamsl) with a median value of 300.47 mamsl. Several trends are evident in the GWE data:

a) There was a sharp decrease in GWE in two monitoring wells immediately after the EVO injection. Values on days 1 and 8 in FW216 were as much as 140 cm below the pre-test value and the value on day 8 in MLSB3 was 80 cm below the pre-test value. Decreases were not observed in any of the other wells and it is likely that the short-term changes measured in FW216 and MLSB3 were errors in readings.

b) GWE values in all wells increased about 20 cm between 10-15 days after the EVO injection and remained at this higher level until about 50 after injection.

c) GWE values in all wells increased about 50 cm between 50 and 78 days after injection. In all but one of the wells (FW212), the values decreased to near the 50 day level by the time of the next measurement (78 days).

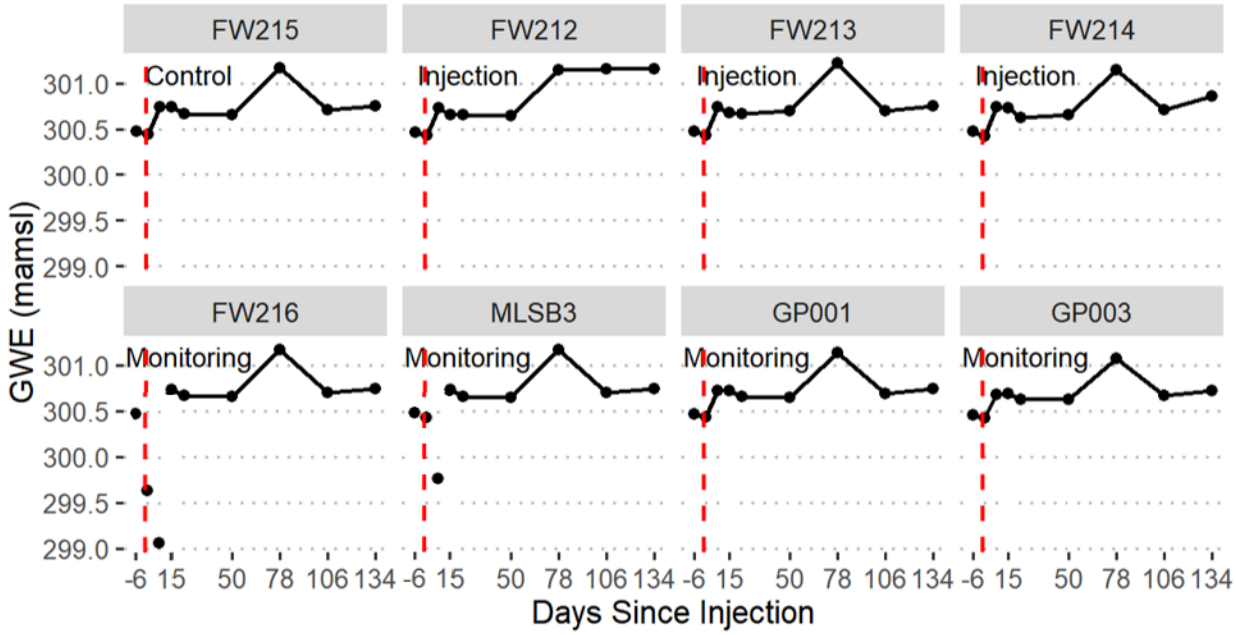


Figure 7. Groundwater elevation (GWE) in meters above mean sea-level (mamsl) during the experiment. The red dashed line represents the day of injection.

d) GWE trends in all of the wells showed the same general trends, with the exceptions of the short-term decreases noted above for FW216 and MLSB3. There were no apparent differences in trends according to well type (control, injection and monitoring).

Precipitation values are shown in **Figure 8**. The rainfall data were typical of winter weather conditions in east Tennessee. During the 134 day period of monitoring, there were 50 days with measurable precipitation. This included 24 days with more than 1 cm of precipitation. There were several periods of heavier rainfall, including from -5 to 10 days, when 8 cm was recorded, from 45 to 78 days, when 25 cm was recorded, and from 125 to 134 days, when 6 cm was recorded. There were also about 6 or 7 days when 1 to 2 cm of precipitation was recorded.

The observed changes in GWE were most likely related to precipitation. The 20 cm rise in GWE noted after day 8 in almost of the wells occurred a few days after a period of heavy rain, which occurred right after the EVO injection. The next large rise in GWE (about 50 cm, in all wells between days 50 and 78) occurred near the end of a period of heavy precipitation, which occurred between 45 and 78 days. There was another smaller rise in GWE (about 10-15 cm) observed in all but one of the wells near the end of the test, which corresponded to another period of heavier rain, from 125 to 134 days. There is no indication that the EVO injection influenced GWE values.

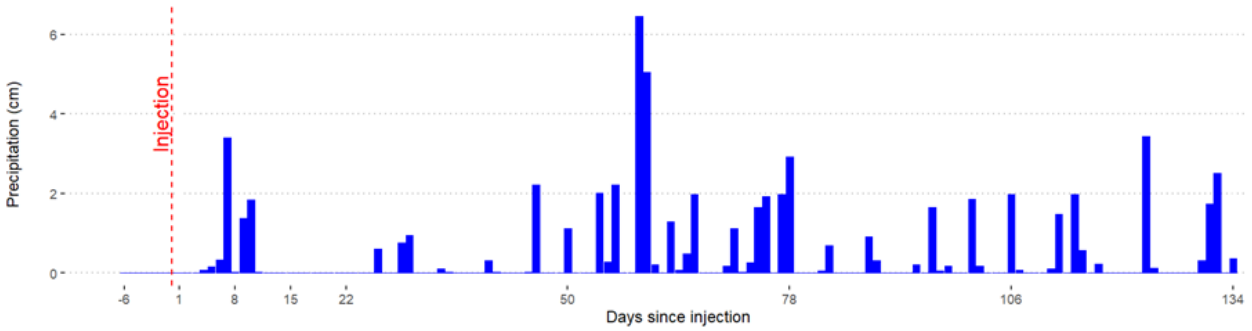


Figure 8. Precipitation from six days before injection until the final day of the experiment. The red dashed line represents the date of injection. The heaviest period of precipitation occurred between day 45 and day 78.

Hydraulic Gradient

All references to hydraulic gradient here refer to the central injection well, FW212, and the monitoring well furthest down-gradient, GP003. Six days before injection, the hydraulic gradient across the study site was very shallow at -0.00022 (-0.02%). The gradient decreased to -0.0033 (-0.33%) following the EVO injection. However, the hydraulic gradient returned to -0.00022 (-0.02%) the following week. On day 15, the hydraulic gradient was positive between FW212 and GP003 at 0.0029 (+0.29%). At day 22, the hydraulic gradient was at -0.002 (-0.2%) and stayed within that range until day 78. By day 106, the hydraulic gradient increased to -0.035 (-3.5%) and was slightly higher than the pre-injection measurements. On the final measurement, 134 days after injection, the hydraulic gradient was -0.031 (-3.1%). Over the course of the experiment, the hydraulic gradient increased from the pre-injection value of -0.02% to -3%. However, given the variability it is unlikely that the EVO caused any significant increase over the course of the injection.

Hydraulic Conductivity

The pumping rates and drawdown used to calculate hydraulic conductivity can be found in **Tables 5 and 6**. Pumping rates required to achieve a steady-state were highly variable throughout the study. In some cases, pumping rates were at the upper limit of the usual criteria set for low-flow sampling of 1 L/min. Steady-state drawdown values were also highly variable, with some values near the limit of reliable measurement using an electric water level tape (approximately 0.3 cm for this study). Drawdown values may be even less reliable than water level values, because they tend to vary during a test and are based on the difference between two water level measurements.

Table 5. Pumping rates and drawdown used to calculate the hydraulic conductivity in injection wells.

Well ID	Days since Injection	Pumping Rate (mL/min)	Drawdown (cm)
FW212	-6	900	0.9
	1	850	0.9
	8	750	4.3
	15	750	4.9
	22	750	5.5
	50	700	19.5
	78	325	30.2
	106	375	1.5
	134	450	6.4
FW213	-6	900	1.2
	1	650	0.9
	8	600	2.7
	15	1000	2.1
	22	650	1.2
	50	600	10.4
	78	325	1.8
	106	425	2.1
	134	550	0.3
FW214	-6	900	3.7
	1	900	5.8
	8	700	18.3
	15	1000	22.9
	22	600	34.4
	50	500	60.0
	78	325	56.4
	106	325	32.3
	134	500	0.9

Table 6. Pumping rates and drawdown used to calculate hydraulic conductivity in the control and monitoring wells.

Well ID	Days since Injection	Pumping Rate (mL/min)	Drawdown (cm)
FW215 (Control)	-6	800	0.6
	1	1000	0.6
	8	750	1.2
	15	1000	0.6
	22	900	1.2
	50	725	0.9
	78	300	0.6
	106	300	0.3
	134	600	0.6
FW216	-6	800	3.7
	1	1000	77.7
	8	825	3.1
	15	950	1.2
	22	750	3.1
	50	750	3.4
	78	390	1.5
	106	400	2.1
	134	575	3.4
MLSB3	-6	900	2.7
	1	1000	19.2
	8	1000	4.6
	15	750	16.5
	22	750	16.5
	50	750	15.5
	78	400	7.6
	106	450	10.1
	134	550	13.4
GP001	-6	900	0.9
	1	950	17.7
	8	100	2.4
	15	800	1.5
	22	900	1.2
	50	550	2.7
	78	400	1.8
	106	425	2.4
	134	525	1.8
GP003	-6	900	0.9
	1	900	0.9
	8	750	1.8
	15	900	1.8
	22	900	1.5
	50	650	1.2
	78	390	1.2
	106	450	0.6
	134	625	1.2

In this study, six of the eight wells had at least one instance where the K value was based on a drawdown of less than 1 cm. For example, in the control well, FW215, drawdown values varied from 0.3 to 1.2 cm, all of which are close to the limit of accurate measurement. In other cases, like monitoring wells GP001 and GP003, as well as injection well FW212, the drawdown values of questionable reliability (0.6 cm or less) occurred in the pre-test measurement, with larger drawdown values typically measured in the post-EVO injection measurements. The uncertainty in measured drawdown values contributes to uncertainty in measured hydraulic conductivity. However, it is still possible to evaluate the possible impact of the EVO injection on hydraulic conductivity by considering any values that are near the limit of measurement reliability as minimum values, with actual values likely being greater than or equal to the measured value. In some cases, typically the injection wells, this means that the observed decline in hydraulic conductivity relative to initial values based on small drawdowns may be even larger than indicated.

Values for hydraulic conductivity measured over the course of the experiment can be found in a faceted graph in **Figure 9**. The pre-test hydraulic conductivity value for the eight wells used in the study varies from 4.1x10-2 to 1.5x10-1 cm/s. This is a relatively narrow range for a heterogeneous fill material, although as previously mentioned, the pre-test hydraulic conductivity in some of the wells may be higher than the measured values due to uncertainty in measuring small drawdown values.

The control well (FW215) did not appear to be negatively impacted by the EVO injection. This was confirmed using a one-sample t-test which reported $p = 0.97$ indicating that

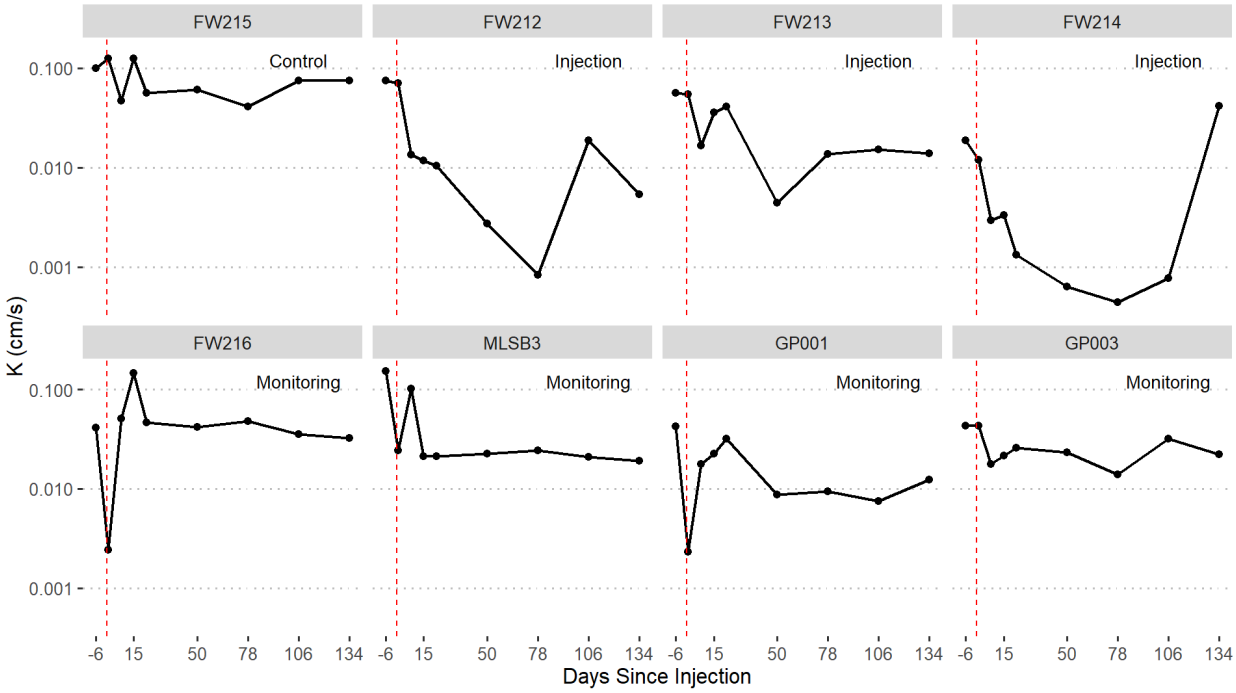


Figure 9. A faceted graph of hydraulic conductivity during the study. Labels within each facet identify the well type. The red dashed line represents the day of injection.

there was no significant difference between the pre-injection value and the post-injection values. The control well generally had the highest values for hydraulic conductivity throughout the entire experiment, staying between $4.08x10^{-2}$ and $1.26x10^{-1}$ cm/s. After day 22, FW215 fluctuated within a relatively small range between $4.08x10^{-2}$ and $7.54x10^{-2}$ cm/s.

All three injection wells (FW212, FW213, FW214) had small reductions in hydraulic conductivity one day after EVO injection, with values decreasing further by day eight. By day 78, injection wells FW212 and FW214 had reductions in hydraulic conductivity nearing two orders of magnitude lower than the pre-test value. Injection well FW213 also had reductions in hydraulic conductivity, however, they were not nearly as large as the FW212 and FW214. FW213 showed a modest increase in hydraulic conductivity on day 22 from its previous post-injection low on day 15. However, the value sharply decreased after that and became stablized, between $1.36x10^{-2}$ and $1.53x10^{-2}$ cm/s, by day 78. Down-gradient monitoring wells also had decreases in hydraulic conductivity following EVO injection, but they tended to be smaller than in the injection wells. However, they rebounded relatively quickly, between days 8 and 15, and their hydraulic conductivity became stable around day 50.

Post-injection hydraulic conductivity values for individual wells were compared to the control well with a paired t-test using normalized data (**Table 7)**. The tests reported that significant differences exist in two of the three injection wells (FW212 and FW213) and in two out of the four down-gradient monitoring wells (MLSB3 and GP001) (**Table 8**). Even though there is an obvious change in hydraulic conductivity in FW214, the test reported $p = 0.2553$. This is likely due to the influence of the large change in hydraulic conductivity in the last measurement where, when normalized, was > 1 and the limitations of statistics small sample

Table 7. Normalized hydraulic conductivity values. Each well has been normalized against the pre-injection value (day -6). Normalization removes the influence of spatial variation and allows for the comparison of change relative to the pre-injection measurement.

Days Since Injection	FW215 (Control)	FW212 (Injection)	FW213 (Injection)	FW214 (Injection)	FW216 (Monitoring)	MLSB3 (Monitoring)	GP001 (Monitoring)	GP003 (Monitoring)
-6	0	0	0	0	0	0	0	0
1	0.2500	-0.0556	-0.0388	-0.3684	-0.9412	-0.8413	-0.9454	0
8	-0.5312	-0.8214	-0.7037	-0.8444	0.2375	-0.3333	-0.5833	-0.5833
15	0.2500	-0.8438	-0.3651	-0.8222	2.5625	-0.8611	-0.4667	-0.5000
22	-0.4375	-0.8611	-0.2778	-0.9298	0.1262	-0.8611	-0.2500	-0.4000
50	-0.3958	-0.9635	-0.9216	-0.9662	0.0227	-0.8529	-0.7963	-0.4583
78	-0.5938	-0.9891	-0.7593	-0.9766	0.1700	-0.8400	-0.7778	-0.6750
106	-0.2500	-0.7500	-0.7302	-0.9591	-0.1429	-0.8636	-0.8229	-0.2500
134	-0.2500	-0.9286	-0.7556	1.2222	-0.2159	-0.8750	-0.7083	-0.4792

Table 8. The reported two-tail p-values of paired t-tests comparing normalized post-injection hydraulic conductivity values of the control well to the other wells used in the study. Statistically significant results have been highlighted in bold.

FW212 (Injection)	FW213 (Injection)	FW214 (Injection)	FW216 (Monitoring)	MLSB3 (Monitoring)	GP001 (Monitoring)	GP003 (Monitoring)
0.0007	**0.0093**	0.2553	0.2134	**0.0088**	**0.0261**	0.0947

sizes. The test was repeated for FW214 without considering the values at day 134 and it showed that a significant difference ($p = 0.009$) existed. This suggests that there was a significant, although transient, reduction in hydraulic conductivity when omitting the outlier on day 134.

A Shapiro-Wilks test determined that values for hydraulic conductivity were not normally distributed. Tukey's Ladder of Powers test determined that a transformation of $K^{0.3}$ would make the data follow a normal distribution. This transformation was applied to the data so they could be compared by well type (control, injection, monitoring) using a one-way ANOVA test. The one-way ANOVA, with transformed post-injection hydraulic conductivity and well type as the factor, resulted in $p < 0.0001$ with a Cohen's F effect size = 0.749 and a statistical power = 0.87 (**Figure 10**). A highly significant difference existed concerning hydraulic conductivity when considering whether the well was subjected to direct injection or not.

Comparisons of post-injection hydraulic conductivity between the control well and individual wells show that there are statistically significant differences. These differences occur in both the injection wells and down-gradient monitoring wells. However, because normalized data was used in these comparisons, the results are not influenced by spatial variation and compare the changes in hydraulic conductivity relative to the pre-injection values. Since the control well was not influenced by the EVO injection, these results suggest that the injection wells and down-gradient monitoring wells likely had their hydraulic conductivity influenced by the injection of EVO. The results of the one-way ANOVA reported a highly significant difference in hydraulic conductivity when considering whether the well was control, injection, or monitoring.

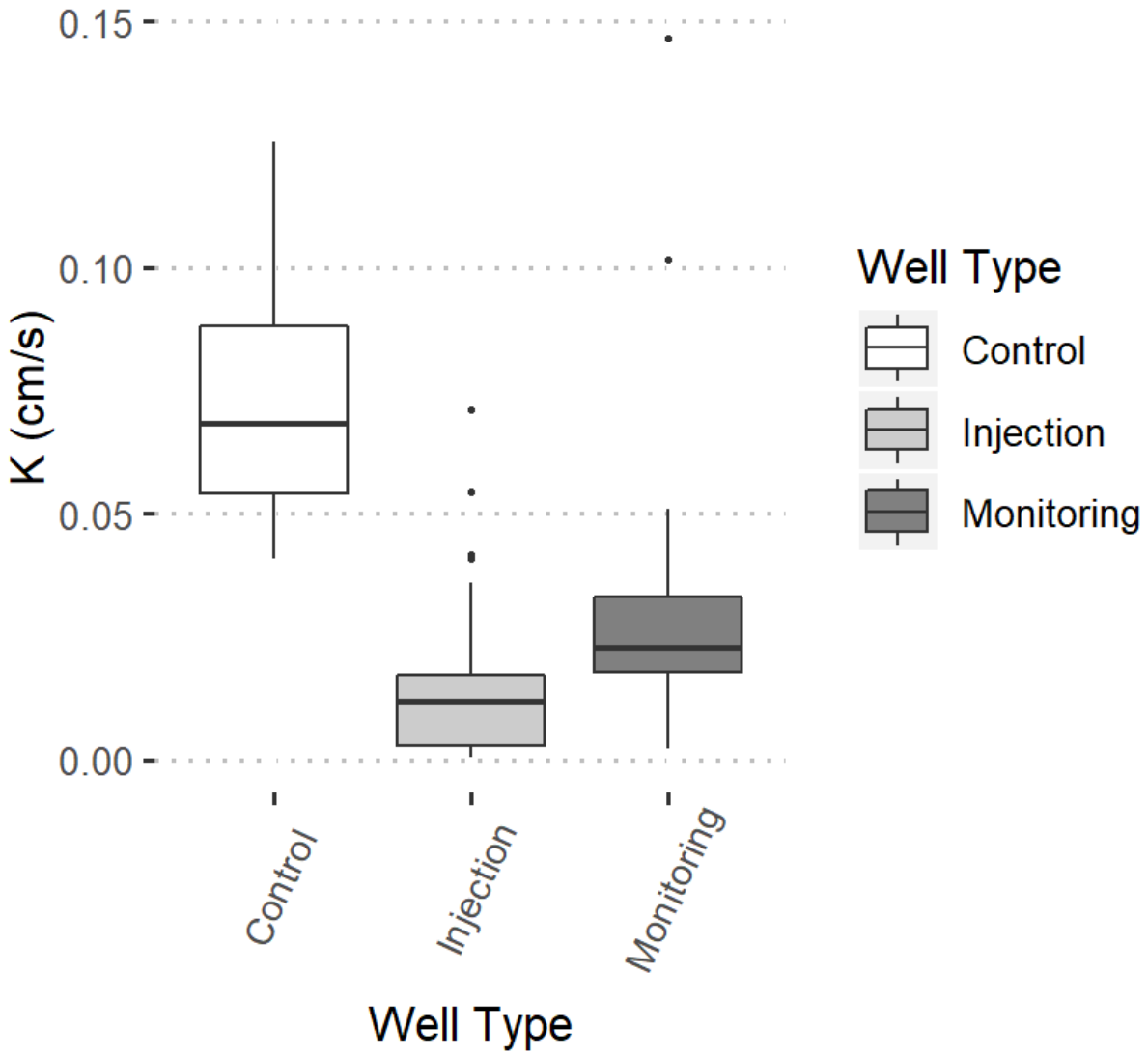


Figure 10. A box and whisker plot of post-injection hydraulic conductivity values by well type. Control, injection, and monitoring wells were all significantly different ($p < 0.0001$) from each other. The control well had the highest average hydraulic conductivity and the injection wells had the lowest average hydraulic conductivity.

Dissolved Uranium Concentrations

Dissolved uranium concentrations in each well over the course of the experiment can be found in a faceted graph in **Figure 11**. Before EVO injection, dissolved uranium concentrations ranged from a minimum value of 715.8 µg/L in injection well FW214 and a maximum of 1111.5 µg/L in monitoring well MLSB3. By day 8 following EVO injection, the dissolved uranium concentrations ranged from 397.8 to 1174.7 µg/L across the site. The lowest concentrations were in injection wells FW212, FW213, and FW214, and the control well FW215 had the highest concentration on day 8. By day 50 post-injection, dissolved uranium concentrations reached the lowest values in all wells, including the injection wells. The control well FW215 and the monitoring well immediately down-gradient from the injection wells, FW216, had the highest concentrations, which were higher than pre-injection. On day 78, dissolved uranium concentrations increased in all wells, except for FW215 and FW216. The measured increases in dissolved uranium may be related to the rainfall that occurred between days 50 and day 78 and the corresponding increase in GWE (**Figures 7 and 8**). Although dissolved uranium concentrations generally began to increase, the injection wells still had the lowest concentrations on the site. The furthest down-gradient monitoring well, GP003, had the highest dissolved uranium concentration measured during the experiment at this time, which was 900 µg/L higher than its pre-injection concentration. At the final time point, 134 days after EVO injection, the injection wells still had low dissolved uranium concentrations. Injection wells were the only wells that were below their pre-injection dissolved uranium concentrations at the end of the experiment. Down-gradient monitoring wells, apart from GP001, had dissolved uranium concentrations that were above their pre-injection values at this time.

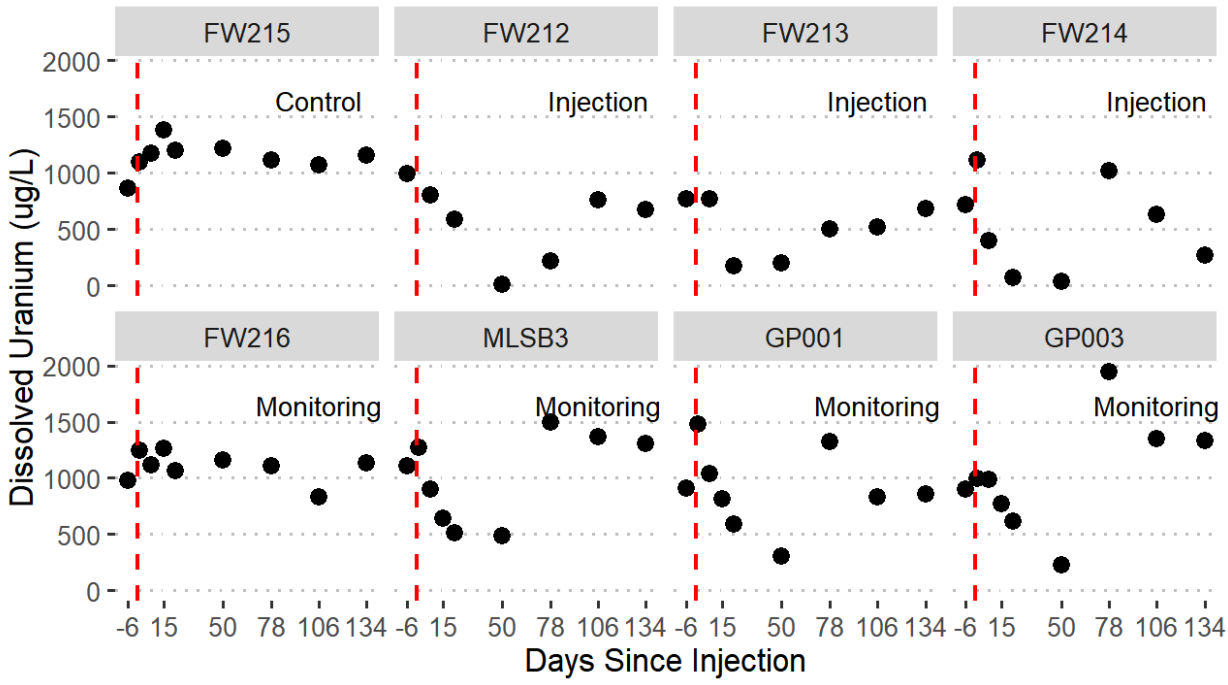


Figure 11. A faceted graph of dissolved uranium concentrations measured during the experiment. Each facet is labeled with the well type. The dashed red line represents the day of injection. Injection wells had concentrations lower than their pre-injection values at the end of the experiment. All monitoring wells were either near their pre-injection concentrations or surpassed them by the end of the study.

A one-sample t-test using normalized dissolved uranium concentrations determined that there was a significant difference ($p < 0.0001$) between the pre-injection and post-injection dissolved uranium concentrations in the control well (FW215). However, when inspecting the raw data and normalized data, it is evident that this significant difference was due to increases in dissolved uranium concentration rather than decreases that would be expected had the well been affected by the EVO injection.

Post-injection dissolved uranium concentrations for individual wells were compared to the control well with a paired t-test using normalized data (**Table 9**). The tests reported that significant differences existed in two of the three injection wells (FW212 and FW213) and in two out of the four down-gradient monitoring wells (FW216 and MLSB3) when compared to the up-gradient control well (**Table 10**). Injection well FW214 had a p-value of 0.0556, which was close to the threshold for statistical difference. Although the test reports that there was no significant difference, inspection of the data suggests that this result was likely due to limitations of the statistical test and the small sample size. Monitoring well FW216 also had a significant difference; however, when inspecting the raw and normalized data, it was apparent that this difference was not related to lower dissolved uranium concentrations. Normalized values for dissolved uranium concentrations in FW216 were almost all >0, indicating increases in dissolved uranium relative to the pre-injection concentration. However, increases in dissolved uranium in the control well were almost all >0.2, so the significant difference was likely related to the differences in an increase of dissolved uranium concentrations. Monitoring well MLSB3 also had a significant difference reported by the test. However, the majority of the normalized values were <1 indicating that these differences were related to the decrease of dissolved uranium

Table 9. Normalized dissolved uranium concentrations. Each well has been normalized against the pre-injection concentration (day -6). Normalization removes the influence of spatial variation and allows for the comparison of change relative to the pre-injection

Days Since Injection	FW215 (Control)	FW212 (Injection)	FW213 (Injection)	FW214 (Injection)	FW216 (Monitoring)	MLSB3 (Monitoring)	GP001 (Monitoring)	GP003 (Monitoring)
-6	0	0	0	0	0	0	0	0
1	0.2733	NA	NA	0.5546	0.2712	0.1455	0.6259	0.1036
8	0.3613	-0.1901	-0.0023	-0.4443	0.1421	-0.0314	0.1484	0.0993
15	0.5989	NA	NA	NA	0.2895	-0.4232	-0.0990	-0.1444
22	0.3907	-0.4084	-0.7683	-0.8953	0.0889	-0.5424	-0.3488	-0.3136
50	0.4167	-0.9914	-0.7354	-0.9501	0.1808	-0.5650	-0.7477	-0.6642
78	0.2956	-0.7846	-0.3484	0.4230	0.1352	0.3437	0.4607	1.1599
106	0.2382	-0.2371	-0.3224	-0.1140	-0.1523	0.2278	-0.0870	0.4985
134	-0.0091	-0.3233	-0.1074	-0.6246	0.1568	-0.3926	0.0868	-0.7016

Table 10. The reported two-tail p-values of paired t-tests comparing normalized post-injection dissolved uranium concentrations of the control well to the other wells used in the study. Statistically significant results have been highlighted in bold.

FW212 (Injection)	FW213 (Injection)	FW214 (Injection)	FW216 (Monitoring)	MLSB3 (Monitoring)	GP001 (Monitoring)	GP003 (Monitoring)
0.0059	**0.0124**	0.0556	**0.0257**	**0.0195**	0.1305	0.2012

concentrations in this well.

A one-way ANOVA with post-injection dissolved uranium concentrations and well type as the factor resulted in a $p < 0.0001$ with a Cohen's f effect size = 0.792 and a statistical power = 0.997 (**Figure 12**). This suggests that a highly significant difference exists in dissolved uranium concentration related to whether the well was injected with EVO.

Injection wells had a large range of dissolved uranium concentrations. Down-gradient monitoring wells also had a large range of concentrations and concentrations were higher than injection wells. Statistically significant differences, related to decreases in dissolved uranium concentration, were found in the injection wells when compared to the control well. A significant difference, related to an increase in dissolved uranium, was also found in the first down-gradient control well, FW216. One down-gradient monitoring well, MLSB3, had a statically significant difference that was related to a decrease in dissolved uranium. Overall, the injection wells can be characterized by their decreases in dissolved uranium, while the control and down-gradient monitoring wells had much smaller changes, and in some cases, increases in their concentrations. The highly significant difference found when comparing dissolved uranium concentrations to well type (control, injection, monitoring) as the factor provides supporting evidence that suggests the differences found were likely related to the injection of EVO.

Post-injection Down-gradient Acetate Concentrations

A total of 19 of the 44 measurements for acetate were below the detection limit (BDL) of 0.5 µM. All wells had measurements below detection limits at some point, and all wells were below detection limits on the day following injection. Detectable values for acetate ranged from a minimum of 0.40 µM to a maximum of 773.13 µM. For all analysis and figures, the detection

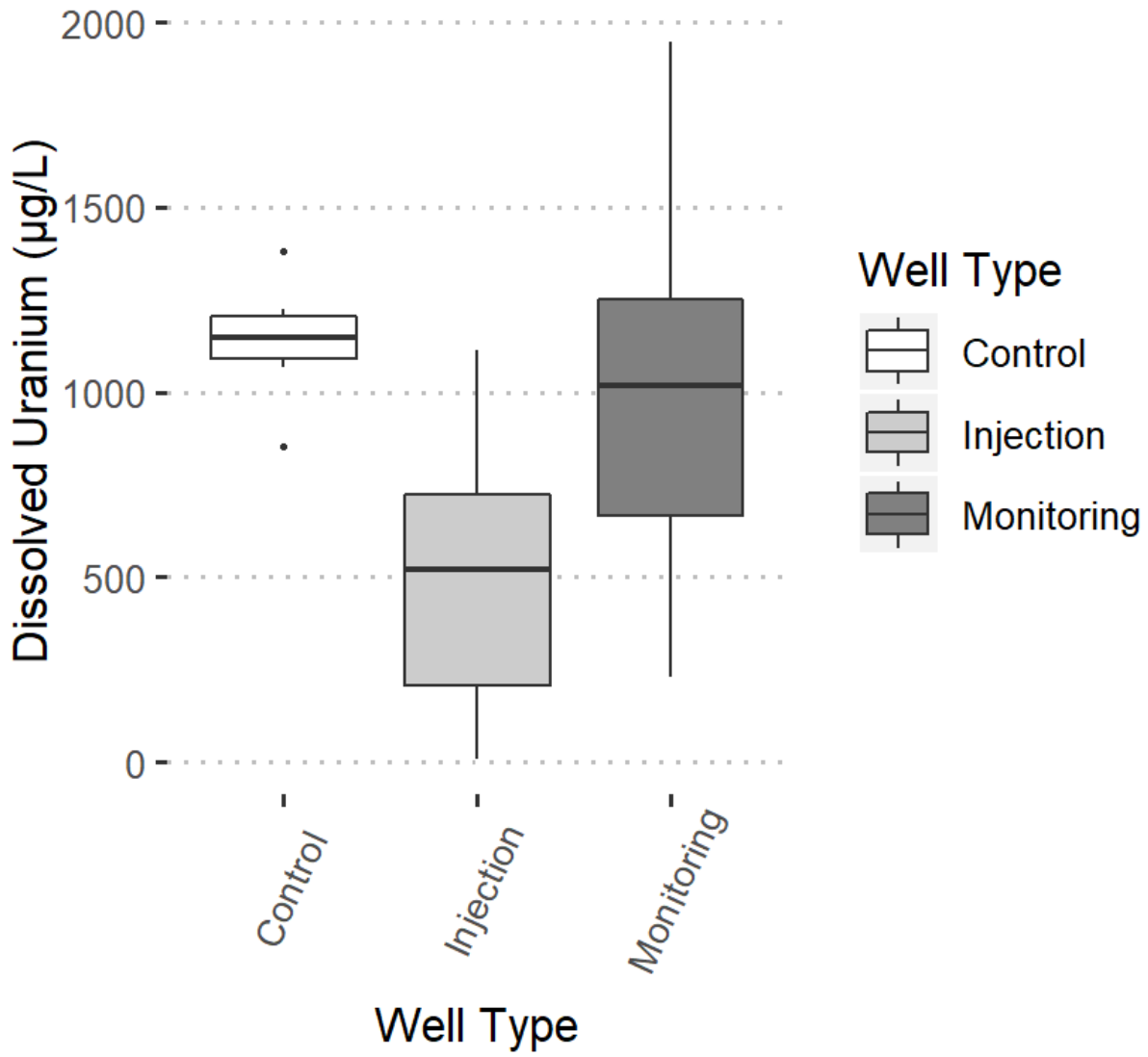


Figure 12. A box and whisker plot of dissolved uranium concentrations by well type. The control well had the highest average concentration and the injection wells had the lowest average concentration during the experiment. Monitoring wells had an average concentration that was approximately 500 µg/L higher than the injection wells.

limit was used in place of values reported as BDL. Due to high concentrations of visible EVO after multiple filtrations and dilution, one sample from GP001 was not able to be analyzed. Acetate concentrations over time can be found in **Table 11**. Both the minimum and maximum acetate concentrations occurred in the monitoring well furthest down-gradient, GP003. By day 8, acetate was detected in all down-gradient wells. The first down-gradient monitoring well, FW216, had a response more similar to the up-gradient control well than with the other monitoring wells. By day 22, all down-gradient monitoring wells had reached their peak acetate concentrations. On day 134, acetate concentration was increased, including in the control well. It is unknown what may have caused this sudden increase.

Acetate concentrations were not normally distributed. Tukey's Ladder of Powers test was applied and failed to find a transformation to bring the data closer to normality. A non-parametric Kruskal-Wallis rank sum test determined that a significant difference did not exist between the control well and down-gradient wells.

An ANOVA test including injection type (primary or secondary), days since injection, and well as factors was used to compare the response of this injection to the most recent 2009 injection in the companion study to this investigation [53]. Acetate was differed significantly by day ($p < 0.001$) and the combination of injection type (primary or secondary) and day ($p = 0.0032$) [53]. These results indicate a significant difference in timing regarding acetate concentrations after amendment injection that is dependent on injection type.

Correlations

Before calculating correlations, all concentrations were converted to µg/L. Kendall correlations computed using the sjt.corr function from the *sjstats* package can be found in **Table 12** [69].

Table 11. Acetate concentrations (µM) in the control and down-gradient monitoring wells over the course of the experiment. An entry of BD means the sample was below the detection limit of the instrument.

Acetate (µM)					
Days Since Injection	FW215 (Control)	FW216 (Monitoring)	MLSB3 (Monitoring)	GP001 (Monitoring)	GP003 (Monitoring)
-6	1.78	1.43	1.59	1.55	BD
1	BD	94.70	610.66	189.67	64.61
8	21.08	BD	494.53	314.32	524.70
15	BD	5.79	274.10	446.82	773.13
22	BD	BD	2.44	91.72	170.39
50	BD	BD	BD	BD	BD
78	BD	BD	BD	BD	BD
106	BD	BD	BD	BD	14.31
134	63.75	70.41	10.00	105.81	256.75

Table 12. A correlation matrix computed using the Kendall method and pair-wise deletions. The number of asterisks indicate significance level (p-value) of the relationship. Three significance levels are present: p-value ≤ 0.0001 (***), p-value ≤ 0.001 (**), and p-value ≤ 0.01 (*). Correlations with p-values ≤ 0.001 are highlighted with bold text.

	Temp (°C)	*pH*	*Eh (volts)*	*Na (µg/L)*	*Mg (µg/L)*	*Al (µg/L)*	*K (µg/L)*	*Ca (µg/L)*	*Fe (µg/L)*	*Mn (µg/L)*	*U (µg/L)*	*Acetate (µg/L)*	*Nitrate (µg/L)*	*Sulfate (µg/L)*
Hyd. Con. (cm/s)	0.098	0.084	0.222*	-0.179*	-0.159	-0.105	0.013	0.218*	-0.133	-0.161	**0.339*****	-0.031	0.062	**0.281****
Temp (°C)		-0.020	0.085	0.232*	**0.258****	-0.105	0.228*	0.014	0.152	**0.260****	0.021	-0.032	-0.072	0.022
pH			-0.016	-0.028	-0.149	-0.171	-0.063	0.105	**-0.264****	-0.150	0.142	0.048	0.033	0.200*
Eh (volts)				0.014	-0.144	0.003	-0.042	**0.249****	-0.067	-0.145	0.095	-0.037	-0.073	0.033
Na (µg/L)					**0.398*****	0.219*	**0.549*****	-0.125	**0.241****	**0.397*****	-0.143	0.022	-0.123	-0.205*
Mg (µg/L)						0.094	**0.238****	-0.050	**0.396*****	**0.999*****	-0.203*	**0.346*****	-0.142	**-0.308*****
Al (µg/L)							**0.264****	**-0.310*****	0.174	0.093	-0.212*	0.019	0.189*	-0.178
K (µg/L)								-0.110	0.229*	**0.237****	-0.033	-0.115	0.105	0.001
Ca (µg/L)									-0.048	-0.051	**0.286****	0.065	-0.142	0.220*
Fe (µg/L)										**0.395*****	-0.231*	0.182	-0.082	-0.164
Mn (µg/L)											-0.204*	0.345*****	-0.143	**-0.310*****
U (µg/L)												-0.245*	0.099	**0.553*****
Acetate (µg/L)													-0.152	**-0.337*****
Nitrate (µg/L)														**0.354*****

Hydraulic conductivity had its largest relationship, according to Cohen's d standards [71], with dissolved uranium (0.339) and a p-value ≤ 0.0001. Hydraulic conductivity also had a large relationship (0.281) with sulfate along with a p-value ≤ 0.001. Hydraulic conductivity also had a small relationship (0.222) with Eh (volts) with a p-value ≤ 0.01. Dissolved uranium concentrations were strongly related (0.553) to sulfate concentrations with a p-value ≤ 0.0001. Nitrate has a strong relationship (0.354, $p \leq 0.0001$) with sulfate, which would be expected due to their relationship as electron acceptors (**Figure 1**). This is also evident in the strong relationship (0.553) between sulfate and uranium. A correlation between dissolved calcium and dissolved uranium (0.286, $p < 0.001$) was also identified. This suggests that increases in dissolved calcium are related to increases in dissolved uranium. This interaction has been identified previously when it was shown that dissolved calcium can inhibit the bacterial reduction of U(VI) [8].

The correlation between hydraulic conductivity and dissolved uranium concentration suggests that when hydraulic conductivity decreased the concentration of dissolved uranium did as well, and vice-versa. Previously discussed results showed that a highly significant difference ($p < 0.0001$) existed in hydraulic conductivity values based on whether the well was injected with EVO. Wells injected with EVO had the lowest hydraulic conductivity post-injection. It was also shown that a highly significant difference ($p < 0.0001$) existed in dissolved uranium concentrations based on whether the well had been injected with EVO which suggests the presence of bioreduction. These results, combined with the strong and significant correlation between hydraulic conductivity and dissolved uranium, suggest that lower hydraulic conductivity in the injection wells was likely related to EVO introduction.

CHAPTER SIX
SUMMARY AND CONCLUSIONS

The results of the tested hypotheses applicable to changes observed over the course of the experiment follow:

i. H_1: The hydraulic conductivity in the injection and down-gradient monitoring wells is lower after EVO injection.

   H_0: There is no difference between pre-injection and post-injection hydraulic conductivity values in the injection and down-gradient monitoring wells.

   The hydraulic conductivity in all three injection and two of the four monitoring wells decreased following EVO injection.

ii. H_1: The hydraulic conductivity in the control well is not lower after EVO injection.

   H_0: The hydraulic conductivity in the control well is lower after EVO injection.

   There was no statistical difference (p = 0.97) in the hydraulic conductivity values of the control well before and after injection.

ii. H_1: The dissolved uranium concentrations in the injection and down-gradient monitoring wells is lower after EVO injection.

   H_0: There is no difference between pre-injection and post-injection dissolved uranium concentrations in the injection and down-gradient monitoring wells.

   The dissolved uranium concentrations in the injection and monitoring wells decreased after the EVO injection.

iii. H_1: Dissolved uranium concentration in the injection and down-gradient monitoring wells are lower than in the up-gradient control well after EVO injection.

H_0: Dissolved uranium concentration in the injection and down-gradient monitoring wells decreases relative to the up-gradient control well after EVO injection.

Significant differences were found for dissolved uranium concentrations in the injection and monitoring wells when compared to the control well. Dissolved uranium concentrations were significantly lower in the injection wells compared to the monitoring wells.

iv. H_1: Hydraulic conductivity affects the concentration of dissolved uranium after EVO injection.

H_0: Hydraulic conductivity does not affect the concentration of dissolved uranium after EVO injection.

Hydraulic conductivity values and dissolved uranium concentrations were significantly correlated to each other (p-value ≤ 0.0001.)

v. H_1: Acetate generation occurring earlier than in the 2009 injection suggests a memory response to the injection of EVO.

H_0: Acetate generation did not occur earlier than in the 2009 injection suggesting that there is no memory response to EVO.

Acetate first appeared in all down-gradient monitoring wells by day 8 post-injection. Peak acetate concentrations occurred in all down-gradient monitoring wells by day

22. Both the appearance in monitoring wells and the peak concentration of acetate occurred earlier than what was observed after the 2009 EVO injection. Acetate was also observed to differ significantly by day ($p < 0.001$) and the combination of injection type (primary or secondary) and day ($p = 0.0032$).

Significant differences were observed in hydraulic conductivity and aqueous uranium concentrations between wells and well types. It is likely that the observed reductions in hydraulic conductivity in the injection wells can mostly be explained by the injection of EVO. This is supported by the significant difference ($p < 0.0001$) reported when comparing hydraulic conductivity with well type, or whether the well was injected with EVO, as the factor.

The relatively large decreases in dissolved uranium concentrations, when compared to the down-gradient monitoring wells, also suggest that much of the injected EVO stayed close to the injection wells. This is supported by significant difference ($p < 0.0001$) in dissolved uranium concentration when considering well type, or whether the well was injected with EVO, as the factor.

Together, the results from hydraulic conductivity and dissolved uranium concentrations suggest that much of the injected EVO stayed near the injection wells and is related to the notably larger decreases in dissolved uranium within those wells. The highly significant correlation ($p < 0.0001$) identified between hydraulic conductivity and dissolved uranium concentrations also supports this conclusion. The relatively large and persistent reductions of hydraulic conductivity in injection wells suggest they were most likely caused by pore throat blockage due to size exclusion of EVO droplets [13]. Increased residual saturation and associated

hydraulic conductivity loss is further exacerbated due to the clay content, which, at this site can be 9% kaolinite [42]. The large surface area of clays and associated negative charge enhance EVO retention.

The observed reductions in hydraulic conductivity likely prevented much of the amendment from dispersing down-gradient from the injection wells. Because a high volume of EVO amendment stayed near the injection sites, these areas could more effectively maintain conditions necessary for bioimmobilization of uranium. The reduced hydraulic conductivity in these wells likely contributed to their lower dissolved uranium concentrations by also limiting potential reoxidation from incoming groundwater. The lowest concentrations of dissolved uranium were observed in the injection wells and coincided with some of the lowest observed hydraulic conductivities. Previous studies showed that excessive reductions in hydraulic conductivity in injection wells can result in contaminated groundwater flowing around the injection site, thus failing the remediation [13]. The subdued response in hydraulic conductivity and aqueous uranium reduction in the up-gradient control well (FW215) and the well immediately down-gradient from the injection wells (FW216) suggests that preferential flow changed after injection and contaminated groundwater likely bypassed the injection wells.

Acetate generation, used as an indicator for EVO degradation, was observed in down-gradient wells earlier than in the 2009 EVO injection. Peak acetate concentration also occurred earlier in down-gradient wells than in the 2009 injection. The increased response by the microbial community, along with the significant difference in timing of acetate generation between the two studies, provides some evidence of a “memory response.” However, the length

of time between injections, approximately 9 years, was likely too long to identify a useful pattern of memory response when using a general electron donor.

Planning biostimulation treatments to bioimmobilize contaminants can be challenging in contaminated areas with significant spatial variations in hydraulic conductivity. A persistent and energy dense electron donor, like EVO, has many attractive properties in the context of biostimulation. However, as shown here, it can also cause unexpected changes in hydraulic conductivity once injected, which can lead to reduced effectiveness or even a failed remediation attempt. Changes in hydraulic conductivity can allow significant volumes of contaminated groundwater to bypass the treatment zone. This can lead to the reoxidation of previously immobilized uranium. These effects are likely to be most prominent when injection wells are closely spaced. Here, wells that were previously installed and used for similar experiments in the past were used as the injection wells. Increased spacing may minimize the overlap of the radius of influence of the EVO once injected. This would likely reduce the effect of the reductions in hydraulic conductivity that can lead to contaminated groundwater bypassing the injection wells. Although the minimizing overlap is likely to be beneficial, having no overlap in the radius of influence between injection wells may result in areas that are unaffected by the EVO injection. These considerations make the use of EVO to bioimmobilize uranium in a sustained fashion more difficult in highly variable hydrogeologic environments. Although other amendments, such as ethanol or acetate, may be less persistent and require more frequent injections to maintain bioimmobilization, they are unlikely to impact preferential groundwater flow in a manner that can increase the chance of reoxidizing immobilized contaminants. In that context, they may be

better suited for highly heterogeneous environments or more effective when used in conjunction with EVO injections.

LIST OF REFERENCES

1. Zhang, P., et al., *Dynamic Succession of Groundwater Sulfate-Reducing Communities during Prolonged Reduction of Uranium in a Contaminated Aquifer.* Environmental Science & Technology, 2017. **51**(7): p. 3609-3620.
2. Watson, D.B., et al., *In situ bioremediation of uranium with emulsified vegetable oil as the electron donor.* Environ Sci Technol, 2013. **47**(12): p. 6440-8.
3. Gihring, T.M., et al., *A limited microbial consortium is responsible for extended bioreduction of uranium in a contaminated aquifer.* Appl Environ Microbiol, 2011. **77**(17): p. 5955-65.
4. Anderson, R.T., et al., *Stimulating the In Situ Activity of Geobacter Species To Remove Uranium from the Groundwater of a Uranium-Contaminated Aquifer.* Applied and Environmental Microbiology, 2003. **69**(10): p. 5884-5891.
5. Borden, R.C., *Effective distribution of emulsified edible oil for enhanced anaerobic bioremediation.* J Contam Hydrol, 2007. **94**(1-2): p. 1-12.
6. Hazen, T.C., *In Situ: Groundwater Bioremediation*, in *Consequences of Microbial Interactions with Hydrocarbons, Oils, and Lipids: Biodegradation and Bioremediation*. 2018. p. 1-18.
7. Wu, W.-m., et al., *Effects of Nitrate on the Stability of Uranium in a Bioreduced Region of the Subsurface.* Environmental Science & Technology, 2010. **44**: p. 5104-5111.
8. Brooks, S.C., et al., *Inhibition of Bacterial U(VI) Reduction by Calcium.* Environmental Science & Technology, 2003. **37**(9): p. 1850-1858.
9. Wolf, D.M., et al., *Memory in microbes: quantifying history-dependent behavior in a bacterium.* PLoS One, 2008. **3**(2): p. e1700.
10. Paradis, C.J., et al., *In situ mobility of uranium in the presence of nitrate following sulfate-reducing conditions.* J Contam Hydrol, 2016. **187**: p. 55-64.
11. Paradis, C.J., et al., *In situ demonstration of sustained adaptation of a natural microbial community to transform substrates*, in *Earth and Planetary Sciences*. 2018, The University of Tennessee.
12. Hazen, T.C., et al., *Deep-Sea Oil Plume Enriches Indigenous Oil-Degrading Bacteria.* Science, 2010. **330**(6001): p. 204-208.
13. Coulibaly, K.M. and R.C. Borden, *Impact of edible oil injection on the permeability of aquifer sands.* J Contam Hydrol, 2004. **71**(1-4): p. 219-37.
14. Hofmanl, J.A.M.H. and H.N. Stein, *Permeability reduciton of porous media on transport of emulsions through them.* Colloids and Surfaces, 1991. **61**: p. 317-329.
15. Clayton, M.H. and R.C. Borden, *Numerical modeling of emulsified oil distribution in heterogeneous aquifers.* Ground Water, 2009. **47**(2): p. 246-58.
16. Saripalli, K.P., et al., *Changes in Hydrologic Properties of Aquifer Media Due to Chemical Reactions: A Review.* Critical Reviews in Environmental Science and Technology, 2001. **31**(4): p. 311-349.
17. Freedman, V.L., K.P. Saripalli, and P.D. Meyer, *Influence of mineral precipitation and dissolution on hydrologic properties of porous media in static and dynamic systems.* Applied Geochemistry, 2002. **(2003)**(18): p. 589-606.

18. Taylor, S.W., P.C.D. Milly, and P.R. Jaffi, *Biofilm Growth and the Related Changes in the Physical Properties of a Porous Medium 2. Permeability.* Water Resources Research, 1990. **26**(9): p. 2161-2169.
19. Shaw, J.C., et al., *Bacterial Fouling in a Model Core System.* Applied and Environmental Microbiology, 1984. **49**(3): p. 693-701.
20. Raiders, R.A., et al., *Selectivity and depth of microbial plugging in Berea sandstone cores.* Journal of Industrial Microbiology, 1986. **1**(3): p. 195-203.
21. Ross, N., et al., *Clogging of a Limestone Fracture by Stimulating Groundwater Microbes.* Wat. Res., 2001. **35**(8): p. 2029 -2037.
22. Brovelli, A., F. Malaguerra, and D.A. Barry, *Bioclogging in porous media: Model development and sensitivity to initial conditions.* Environmental Modelling & Software, 2009. **24**(5): p. 611-626.
23. Cusack, F., et al., *Field and laboratory studies of microbial/fines plugging of water injection wells: Mechanisms, diagnosis, and removal.* Journal of Petroleum Science and Engineering, 1987. **1**: p. 39-50.
24. Konzuk, J., et al. *Creation of Passive Biobarriers Using Emulsified Oil: A Summary of Multiple Field Applications*. in *Eight International In Situ and On-Site Bioremediation Symposium*. 2005. Baltimore, Maryland: Battelle Press, Columbus, OH.
25. Wiesner, M.R., M.C. Grant, and S.R. Hutchins, *Reduced Permeability in Groundwater Remediation Systems: Role of Mobilized Colloids and Injected Chemicals.* Environ Sci Technol, 1996(30): p. 3184-3191.
26. Torkzaban, S., et al., *Colloid release and clogging in porous media: Effects of solution ionic strength and flow velocity.* J Contam Hydrol, 2015. **181**: p. 161-71.
27. Ramachandran, V. and H.S. Fogler, *Plugging by hydrodynamic bridging during flow of stable colloidal particles within cylindrical pores.* Journal of Fluid Mechanics, 1999. **385**: p. 129-156.
28. Zijl, W., *Scale aspects of groundwater flow and transport systems.* Hydrogeology Journal, 1999. **7**(1): p. 139-150.
29. Ameli, A.A., J.J. McDonnell, and K. Bishop, *The exponential decline in saturated hydraulic conductivity with depth: a novel method for exploring its effect on water flow paths and transit time distribution.* Hydrological Processes, 2016. **30**(14): p. 2438-2450.
30. Hazen, T.C., *Biostimulation*, in *Handbook of Hydrocarbon and Lipid Microbiology*. 2010. p. 4517-4530.
31. Zhang, P., et al., *Dynamic Succession of Groundwater Functional Microbial Communities in Response to Emulsified Vegetable Oil Amendment during Sustained In Situ U(VI) Reduction.* Appl Environ Microbiol, 2015. **81**(12): p. 4164-72.
32. Newsome, L., K. Morris, and J.R. Lloyd, *The biogeochemistry and bioremediation of uranium and other priority radionuclides.* Chemical Geology, 2014. **363**: p. 164-184.
33. Thomas, J.M. and C.H. Ward, *In situ biorestoration of organic contaminants in the subsurface.* Environ Sci Technol, 1989. **23**(7): p. 760 - 766.
34. Soo, H. and C.J. Radke, *A filtration model for the flow of dilute stable emulsions in porous media: I. Theory.* Chemical Engineering Science, 1986. **41**: p. 263-272.

35. Soo, H. and C.J. Radke, *A filtration model for the flow of dilute stable emulsions in porous media: I. Parameter evaluation and estimation.* Chemical Engineering Science, 1986. **41**: p. 273-281.
36. Coulibaly, K.M., M.L. Cameron, and R.C. Borden, *Transport of Edible Oil Emulsions in Clayey Sands: One-Dimensional Column Results and Model Development.* Journal of Hydrologic Engineering, 2006. **11**(3): p. 230-237.
37. Jung, Y., K.M. Coulibaly, and R.C. Borden, *Transport of Edible Oil Emulsions in Clayey Sands: 3D Sandbox Results and Model Validation.* Journal of Hydrologic Engineering, 2006. **11**(3): p. 238-244.
38. Soo, H. and C.J. Radke, *The flow mechanism of dilute stable emulsions in porous media.* Ind. Eng. Chem. Fundam., 1984. **23**: p. 342-347.
39. W. Jr. Fetter, C., *Applied Hydrogeology*. 2001, Upper Saddle River, N.J.: Prentice Hall. 598.
40. Saripalli K., P., et al., *Prediction of Diffusion Coefficients in Porous Media Using Tortuosity Factors Based on Interfacial Areas.* Ground Water, 2002. **40**(4): p. 346 - 352.
41. Dijk, P. and B. Berkowitz, *Precipitation and dissolution of reactive solutes in fractures.* Water Resources Research, 1998. **34**(3): p. 457-470.
42. Watson, D.B., et al., *The Oak Ridge Field Research Center Conceptual Model*, U.S.D.o. Energy, Editor. 2004.
43. Paradis, C.J., et al., *Push-pull tests for estimating effective porosity: expanded analytical solution and in situ application.* Hydrogeology Journal, 2017. **26**(2): p. 381-393.
44. Moon, J.W., et al., *Physicochemical and mineralogical characterization of soil-saprolite cores from a field research site, Tennessee.* J Environ Qual, 2006. **35**(5): p. 1731-41.
45. Tang, G., et al., *U(VI) Bioreduction with Emulsified Vegetable Oil as the Electron Donor – Model Application to a Field Test.* Environmental Science & Technology, 2013. **47**(7): p. 3218-3225.
46. Tang, G., et al., *U(VI) bioreduction with emulsified vegetable oil as the electron donor--microcosm tests and model development.* Environ Sci Technol, 2013. **47**(7): p. 3209-17.
47. McKay, L.D., A.D. Harton, and G.V. Wilson, *Influence of Flow Rate on Transport of Bacteriophage in Shale Saprolite.* Journal of Environmental Quality, 2002. **31**(4): p. 1095-1105.
48. Wilson, G.V., J.M. Alfonis, and P.M. Jardine, *Spatial dependency and scaling of subsurface hydraulic properties.* Soil Sci. Soc. Am. J. , 1989(53): p. 679-685.
49. Connell, J.F. and Z.C. Bailey, *STATISTICAL AND SIMULATION ANALYSIS OF HYDRAULIC-CONDUCTIVITY DATA FOR BEAR CREEK AND MELTON VALLEYS, OAK RIDGE RESERVATION, TENNESSEE*, U.S.G. SURVEY, Editor. 1989: Nashville, Tennessee.
50. Webster, D.A. and M.W. Bradley, *Hydrology of the Melton Valley radioactive-waste burial grounds at Oak Ridge National Laboratory, Tennessee*. 1988, ; Geological Survey, Denver, CO (United States). p. Medium: ED; Size: 123 p.
51. Green, S.J., et al., *Denitrifying bacteria from the genus Rhodanobacter dominate bacterial communities in the highly contaminated subsurface of a nuclear legacy waste site.* Appl Environ Microbiol, 2012. **78**(4): p. 1039-47.

52. Smith, M.B., et al., *Natural Bacterial Communities Serve as Quantitative Geochemical Biosensors.* mBio, 2015. **6**(3).
53. McBride, K.R., *Microbial Memory Response: Observing History-Dependent Adaptation to Repeated Exposures of Emulsified Vegetable Oil in a Contaminated Aquifer*, in *Microbiology*. 2018, The University of Tennessee, Knoxville. p. 86.
54. Einarson, M.D. and J.A. Cherry, *A New Multilevel Ground Water Monitoring System Using Multichannel Tubing.* Groundwater Monitoring & Remediation, 2002. **22**(4): p. 52-65.
55. Wu, W.M., et al., *Surge block method for controlling well clogging and sampling sediment during bioremediation.* Water Res, 2013. **47**(17): p. 6566-73.
56. Brodie, E.L., et al., *Microbial community response to addition of polylactate compounds to stimulate hexavalent chromium reduction in groundwater.* Chemosphere, 2011. **85**(4): p. 660-5.
57. Robbins, G.A., A.T. Aragon-Jose, and A. Romero, *Determining hydraulic conductivity using pumping data from low-flow sampling.* Ground Water, 2009. **47**(2): p. 271-86.
58. Aragon-Jose, A.T. and G.A. Robbins, *Low-Flow Hydraulic Conductivity Tests at Wells that Cross the Water Table.* Groundwater, 2011. **49**(3): p. 426-431.
59. Puls, R.W. and M.J. Barcelona, *Low-flow (minimal drawdown) Ground-water Sampling Procedures*, U.S. EPA, Editor. 1996, US EPA: Ada, Oklahoma.
60. U.S. EPA, R., *Low stress (low flow) purging and sampling procedure for the collection of ground water samples from monitoring wells.*, U.S. EPA, Editor. 1996: Boston, Massachusetts.
61. Gu, B., et al., *Geochemical reactions and dynamics during titration of a contaminated groundwater with high uranium, aluminum, and calcium.* Geochimica et Cosmochimica Acta, 2003. **67**(15): p. 2749-2761.
62. Louie, H., et al., *A study of techniques for the preservation of mercury and other trace elements in water for analysis by inductively coupled plasma mass spectrometry (ICP-MS).* Analytical Methods, 2012. **4**(2): p. 522-529.
63. R Core Team, *R: A language and environment for statistical computing.* 2018, R Foundation for Statistical Computing: Vienna, Austria.
64. RStudio Team, *RStudio: Integrated Development for R.* 2015, RStudio, Inc.: Boston, MA.
65. Mangiafico, S., *rcompanion: Functions to Support Extension Eductation Program Evalution*. 2018.
66. Ross, A. and V.L. Willson, *One-Sample T-Test*, in *Basic and Advanced Statistical Tests: Writing Results Sections and Creating Tables and Figures*, A. Ross and V.L. Willson, Editors. 2017, SensePublishers: Rotterdam. p. 9-12.
67. Ross, A. and V.L. Willson, *Paired Samples T-Test*, in *Basic and Advanced Statistical Tests: Writing Results Sections and Creating Tables and Figures*, A. Ross and V.L. Willson, Editors. 2017, SensePublishers: Rotterdam. p. 17-19.
68. Kruskal, W.H. and W.A. Wallis, *Use of Ranks in One-Criterion Variance Analysis.* Journal of the American Statistical Association, 1952. **47**(260): p. 583-621.
69. Lüdecke, D., *sjstats: Statistical Functions for Regression Models*. 2018.

70. Kendall, M.G., *A NEW MEASURE OF RANK CORRELATION*. Biometrika, 1938. **30**(1-2): p. 81-93.
71. Cohen, J., *A power primer*. Psychol Bull, 1992. **112**(1): p. 155-9.

VITA

Benjamin G. Adams was born in Hampton, VA, on May 11th, 1983. He graduated from Morristown West High School in Morristown, Tennessee, in 2001. Benjamin served in the United States Army for four years as an Intelligence Analyst. During his enlistment, he attended rotations at both national training centers, NTC and JRTC, before deploying with the 1st Calvary Division, 4 BCT, 2-12 Battalion during Operation Iraqi Freedom. After returning from deployment and reaching the end of his service obligation, he was honorably discharged.

Benjamin then used his GI Bill to attend Pellissippi State University in Knoxville, Tennessee, where he received an Associates of Science. He continued to use his GI Bill at the University of Tennessee and received a Bachelor of Science in Geology in 2015. In January 2016, he entered a graduate program through the Department of Earth and Planetary Sciences at the University of Tennessee, Knoxville, with Dr. Terry Hazen as his primary advisor. He completed the requirements of a Master of Science degree in the Spring semester of 2019.